Thesis for the Master's degree in Molecular Biosciences
Main field of study in physiology

Julie Staurseth

PGC-1β's role in the regulation of adult mice muscle plasticity

60 study points

Department of Molecular Biosciences
Faculty of Mathematics and Natural sciences
UNIVERSITY OF OSLO November 2009

Acknowledgment

This work presented in this M.Sc. thesis was performed at the Program of Physiology, Department of Molecular Biosciences (IMBV), Faculty of Mathematics and Natural Science, University.

First, I would like to thank Professor Kristian Gundersen for the opportunity to work on this project in his group. It has been a good experience, and I'm grateful for all the guidance and help.

I would like to thank PhD student Ida Gjervold Lund for taking the role of my "co-supervisor". For always being positive, helpful and patient. Your support and guidance have been greatly appreciated, and without you this would not have been possible.

I am also very thankful for all the help provided by Dr. Zaheer A. Rana, Dr. Jo C. Bruusgaard and PhD student Siobhan Anton concerning the practical and theoretical part of my thesis.

I would also like to thank my "partner in crime", Einar, for always making me smile and for helping me through the lab and writing processes. Thanks to the rest of the group, especially Siobhan and Ingrid for making my time here fun, both scientifically and non-scientifically.

To all my friends, especially Tina, Pernille, Isabelle and Rønnaug, thank you for always being there through good times and bad, for helping and supporting me, for making me laugh and cry, and for always reminding me that there are other things in life more important than school.

Last, but not least, I would like to thank Joakim and my family for being understanding, encouraging and patient.

Oslo, November 2009

_____

Julie Staurseth

Abstract

Adult skeletal muscle fibers show an ability to undergo phenotypic alterations without cell death or regeneration in response to environmental changes. Important factors affecting the metabolic and contractile properties of a muscle fiber includes the activation of genes involved in mitochondrial biogenesis and oxidative phosphorylation, as well as fast and slow isoforms of contractile proteins.

The coactivator peroxisome proliferator-activated receptor (PPAR) gamma coactivator (PGC)-1β has recently been proposed to initiate these processes by altering oxygen capacity and myosin heavy chain (MyHC) expression in individual muscle fibers in transgenic animals. However, it is difficult to know if the observed effects reflect a true adult plasticity, or an effect of PGC-1β overexpression throughout myognesis. Here we compared wild type expression patterns of PGC-1β in both fast and slow muscles and investigated the effect of PGC-1β on fiber phenotype in adult mice, where developmental factors are not involved.

Expression patterns of the endogenous PGC-1β protein were analyzed by subcellular protein fractionation and Western blotting, while overexpression was studied by electroporating a plasmid encoding Flag-PGC-1β into both the slow oxidative *soleus* (SOL) and the fast glycolytic *extensor digitorum longus* (EDL). MyHC fiber type distribution was further analyzed among the transfected fibers, and compared to control fibers within the same muscles.

The endogenous PGC-1β protein was found to be expressed 36-fold higher in nuclei from EDL than nuclei from SOL. Overexpression studies in SOL resulted in no MyHC alterations in the PGC-1β-transfected fibers. In EDL an increase in 2x fibers at the expense of 2b fibers was seen when comparing PGC-1β-transfected fibers with the sham-transfected fibers. However, sham transfection in EDL also influenced fiber type, a finding we attribute to selective transfection of fibers with low input resistance. Therefore these findings should be interpreted with caution, and the experiments should be repeated under conditions where sham transfection has no effect.

Table of contents

1. INTRODUCTION

1.1 Skeletal muscle

Skeletal muscle is a complex and heterogeneous system, which shows an enormous variability in its functional features, such as force production, resistance to fatigue, and energy metabolism (Berchtold *et al.*, 2000). Skeletal muscles primarily obtain this heterogeneity during development, when immature myoblasts differentiate into the long, cylindrical, multinucleated fibers (cells) that make up the skeletal muscle. These fibers exhibit different functional properties so that groups of fibers or muscles can face tasks ranging from steady low-level activities, such as maintenance of posture, to sudden bursts of intense activity, such as rapid movements or resistance training (Arany, 2008).

Most mammalian muscles consist of a mixture of the different fiber types, and this diversity is related to the expression of different isoforms of contractile and metabolic proteins in the muscle. Muscle fibers are mainly classified according to two major functional characteristics, their speed of contraction and their ability to resist fatigue.

Skeletal muscle diversity was realized as early as in 1874 when it was established that muscles differed in color, red or white (Ranvier, 1874). In the early 19th century the correlation between color and speed of contraction was confirmed (Paukal, 1904), in which slow-contracting muscles (such as *soleus* (SOL)) are always red, in contrast to fast-contracting muscles (such as *extensor digitorum longus* (EDL)), which can be either red or white (reviewed in Needham, 1926). Today we know that color of skeletal muscle is due to the amount of myoglobin (Kendrew *et al.*, 1954), a red oxygen-binding pigment, which correlates with the oxygen capacity of the muscle.

Muscle fibers' speed of contraction correlates with the myosin molecules' ability to hydrolyze adenosine triphosphate (ATP) via their myosin ATPase (mATPase). The greater intrinsic speed, the higher the ATPase activity of the respective muscle. This was originally shown by Barany (1967), and in 1985 Reiser *et al.*(1985) showed that the shortening velocity of individual fibers correlate with the myosin heavy chain (MyHC) isoform composition, but did not show any consistent correlation with myosin light chain (MyLC) isoforms. Fiber type-

specific programs of gene expression are not restricted to just the MyHC isoforms, but exist for other muscle proteins as well (Schiaffino & Reggiani, 1996; Pette & Staron, 1997; Windisch *et al.*, 1998), such as troponin subunits, tropomyosin, α-actinin, and various Ca^{2+}-regulatory proteins such as sarco/endoplasmic reticulum Ca^{2+}-ATPase (SERCA), dihydropyridine (DHP)-receptor and calsequestrin (Pette & Staron, 1993, 1997). All of these may contribute to a faster contraction and a shorter duration time. The different isoforms may be expressed in a graded fashion; the fast Ca^{2+}-ATPase isoform SERCA1 is expressed at higher levels in type 2b fibers compared to type 2a fibers, or in an all or none fashion; e.g. phospholamban is found in type 1, but not in type 2 fibers (Pette & Staron, 1993, 2000).

With histochemical procedures three main fiber types, termed type 1, 2a and 2b were discovered as a result of mATPase activity (Brooke & Kaiser, 1970). Later with the development of immunohistochemical techniques and monoclonal anti-MyHC antibodies (Schiaffino *et al.*, 1986), a fourth MyHC fiber type, the 2x fiber, expressing MyHC isotype 2x was identified (Schiaffino *et al.*, 1989; DeNardi *et al.*, 1993). This fiber type was classified as an intermediate between 2a and 2b fibers, by being relatively oxidative compared to 2b (Larsson *et al.*, 1991) and more fast-twitch than 2a (Bottinelli *et al.*, 1994). In total, 11 different MyHC isoforms in adult mammalian muscles encoded by separate genes have been identified (Pette & Staron, 2000). Four of these, MyHC 1, 2a, 2x, and 2b, are present in adult rodent limb muscles (Brooke & Kaiser, 1970; Schiaffino *et al.*, 1989).

Usually, only one isoform is expressed in each fiber at a time, but the co-expression of different MyHC genes, e.g., fibers containing both 1 and 2a-MyHC, 2a and 2x-MyHC, 2x and 2b-MyHC occur (Pette & Staron, 1990; Schiaffino & Reggiani, 1994). Although hybrid fibers are often assumed to represent a negligible population, substantial data indicates that a considerable percentage of these fibers are present in normal adult muscles (e.g. Biral *et al.*, 1988; Schiaffino & Reggiani, 1994). These hybrid fibers generally show an intermediate mean cross-sectional area (CSA), succinate dehydrogenase (SDH) and α-glycerolphosphate dehydrogenase (GPD) values lying between their respective pure MyHC fiber types, suggesting a continuum of contractile and metabolic properties from type 2b to type 1 (Rivero *et al.*, 1998).

There is a correlation between muscle fibers speed of contraction and their ability to resist fatigue; with slow twitch fibers being oxidative and fast twitch fibers being glycolytic. Type 1 is believed to be the most fatigue resistant fiber type, due to high concentrations of mitochondria and oxidative enzymes (e.g., SDH), while 2b fibers are fast fatigable due to low concentrations of mitochondria, but have high concentrations of glycogen and glycolytic enzymes (e.g., GPD). When comparing speed of contraction, 2b fibers are the fastest due to fast hydrolysis of ATP, this however, is only a short-lasting source of ATP since the amount of substrate is limited; while type 1 fibers have the slowest hydrolysis (Schiaffino & Reggiani, 1994). Type 2a and 2x show intermediate speed of contraction, resistance to fatigue, and metabolic profile compared to type 1 and 2b. An overview of the physiological properties of the different MyHC isoforms is presented in table 1.1. An inverse relationship between CSA and SDH activity has been proven, as well as a relationship between CSA and MyHC, with the ranking order 1/2a-2a/1-2x-2b (Sieck *et al.*, 1995; Delp & Duan, 1996; Rivero *et al.*, 1998). However, since the range in fiber size varies both within and between the different fiber types, among different muscles, and among different strains of rat and mice, it is difficult to make up a define scheme of the relationship between CSA, SDH and MyHC.

Table 1.1 An overview of the fiber types defined by MyHC isoform and physiological properties in skeletal limb muscle of rodents.

Fiber type:	MyHC:	Speed of contraction:	Metabolic profile:	Endurance:
1	MyHC 1	Slow	Oxidative	Good
2a	MyHC 2a	Fast	Oxidative-glycolytic	Good-Medium
2x	MyHC 2x	Faster	Glycolytic-oxidative	Medium-poor
2b	MyHC 2b	Fastest	Glycolytic	Poor

Myosin heavy chain (MyHC) expression determines the muscle fiber type and defines the speed of contraction. Resistance to fatigue, and the metabolic profile defines the level of endurance.

The most frequently used muscles in studies concerning fiber type and metabolic profile are the fast glycolytic EDL and the slow oxidative SOL. This is due to their extreme phenotypes in mice (table 1.2) and rat (data not shown).

Table 1.2 Fiber type frequency (%) of a typical fast muscle (EDL) and a typical slow muscle (SOL).

Muscle:	Animal:	1	2a	2x	2b	Reference:
EDL	Mouse	1	12	19*	68	(Hughes *et al.*, 1999)
EDL	Mouse	1	54	-	45	(Wernig *et al.*, 1989)
SOL	Mouse	50	50	0	0	Ekmark unpub,
SOL	Mouse	55	51	0*	0	(Hughes *et al.*, 1999)

Extensor digitorum longus (EDL) muscle in mice is predominated by fast glycolytic muscle fibers (2b), while slow oxidative muscle fibers dominate in the *soleus* (SOL) (1 and 2a). *2x fiber frequencies are calculated assuming 1 + 2a + 2b + 2x = 100 % (Hughes *et al.*, 1999). – Not measured (Wernig *et al.*, 1989).

1.2 Plasticity of muscle fiber phenotype

Even though the basic fiber type composition of a muscle is largely determined during development, the adult muscle retains its ability to undergo substantial phenotypic alterations (Pette, 2002; Schiaffino *et al.*, 2007) as a response to changes in the environment, e.g. nerve activity, mechanical stimuli, hormonal activity and aging (Pette & Vrbova, 1985; Gorza *et al.*, 1988; Pette & Staron, 1997; Mercier *et al.*, 1999; Pette & Staron, 2000). The phenotypic alterations occur in fully differentiated cells from slow/oxidative to fast/glycolytic and vice versa, without cell death or regeneration (Gorza *et al.*, 1988; Personius & Balice-Gordon, 2001). This transition in MyHC isoform expression occurs in a sequential and reversible order: MyHC 1 ↔ MyHC 2a ↔ MyHC 2x ↔ MyHC 2b (Windisch *et al.*, 1998; Pette & Staron, 2000). During this transition the percentage of hybrid fiber populations often increases (Pette & Staron, 1997, 2000).

The firing pattern of the motor neuron that innervates the muscle has been shown to have the most profound effect. This was demonstrated in a series of classic experiments, starting with the cross-innervation experiments by Buller *et al.* (1960), which demonstrated that innervated slow muscles became fast when re-innervated with a fast nerve and vice versa for fast muscles (reviewed in Pette & Vrbova, 1985). This resulted in two main hypotheses of how the nerve conducted these changes, by electrical signals and/or neurotrophic factors secreted from the nerve. Several studies have shown that when stimulating the denervated muscle directly by steel electrodes, thereby excluding trophic factors, electrical signals alone are sufficient to change the properties of the muscle in the same way as the cross-innervated muscles. Slow contraction speed and high fatigue resistance was induced in the fast EDL muscle when

stimulated with a slow electrical stimulation pattern (chronic, low-frequency), inducing fast-to-slow transformation (e.g. Eken & Gundersen, 1988; Westgaard & Lomo, 1988; Gundersen & Eken, 1992). Slow-to-fast transformation was achieved when stimulating the slow SOL muscle with high frequency stimulations, resulting in a less fatigue resistant muscle (e.g. Lomo *et al.*, 1974; Gorza *et al.*, 1988; Gundersen & Eken, 1992). The importance of electrical signals has been well established, while the role of the neurotrophic factors, if they exist, are still somewhat unclear.

Endurance training, or prolonged low-frequency muscle activity, might induce fast-to-slow fiber type-switch by increasing the oxidative metabolism through expansion of the mitochondrial compartment and increased angiogenesis (e.g. reviewed in Arany, 2008). This improves endurance and resistance to fatigue. Stretch and mechanical load has been shown to cause the same transition (Pattullo *et al.*, 1992). In contrast, mechanical unloading has shown transition in a faster direction (Vrbova, 1963; Jankala *et al.*, 1997).

Inactivity, decreased activity, severe malnutrition or disease may cause atrophy (reduced CSA) in the muscle and induces a slow-to-fast transformation (Pette & Staron, 2000; Arany, 2008).

Aging is associated with decrease in total muscle CSA (atrophy) as a result of a reduction in the number of muscle fibers and a reduction in the CSA of individual fibers (Lexell *et al.*, 1988). However, in contrast to disease, inactivation and decreased activity, aging induces a fast-to-slow transformation (Larsson & Ansved, 1995; Pette & Staron, 2000). This is a result of selective decrease in muscle fiber size; type 2 fibers decrease with increasing age, whereas type 1 fibers are unaffected (Roos *et al.*, 1997). The relative contribution of type 2 fibers to force generation is therefore less in the aged than in the young. There is also evidence for selective atrophy of type 2 fibers (Klitgaard *et al.*, 1989; Klitgaard *et al.*, 1990); however, the literature presents conflicting evidence about whether the loss of muscle fibers are type-specific or not (Lexell *et al.*, 1986; Lexell, 1993), which is the main factor for a decreased total muscle CSA (Roos *et al.*, 1997).

Different hormones (Izumo *et al.*, 1986; Moxley, 1994; Van Zyl *et al.*, 1995) have a profound effect on muscle fiber composition, energy metabolism and protein synthesis in fast and slow skeletal muscles. The thyroid hormone appears to have the greatest effect on muscle fiber type.

In general, hypothyroidism causes an increase in slow fibers, whereas hyperthyroidism elicits transition in the opposite direction (Ianuzzo *et al.*, 1977; Nwoye & Mommaerts, 1981; Pette & Staron, 1997). Other hormones, such as testosterone, may contribute to gender differences in fiber size, affecting the relative concentrations of MyHC isoforms in young untrained men and women (Staron *et al.*, 2000).

However, the signaling pathways linking muscle activity to alterations in gene expression of the metabolic and contractile proteins are far from fully understood. Recently published literature suggests that an array of signaling pathways, rather than a "master" switch or pathway, are responsible for the changes in fiber phenotype seen in adult skeletal muscle (Spangenburg & Booth, 2003; Koulmann & Bigard, 2006).

1.3 Signaling pathways regulating muscle plasticity

Several independent signaling pathways regulating skeletal muscle phenotype have so far been identified. Only a few of these pathways have been proposed as regulators linking electrical signals from motor neurons to a fast glycolytic phenotype (Seward *et al.*, 2001; Grifone *et al.*, 2004; Noirez *et al.*, 2006; Ekmark *et al.*, 2007). MyoD knockout mice express low levels of MyHC 2b messenger ribonucleic acid (mRNA) when compared to muscles of wild type mice (Seward *et al.*, 2001). Somatic MyoD deoxyribonucleic acid (DNA) transfer in adult mice has shown elevated levels of MyHC 2b (Ekmark *et al.*, 2007). Another mechanism, the Six and Eyes absent homolog (Eya) pathway, is involved in the establishment and maintenance of a fast-twitch muscle phenotype (Grifone *et al.*, 2004). Pathways regulating slow-gene programs are more extensively investigated.

Myogenin was found, when overexpressed in transgenic mice, to increase oxidative capacity and decrease fiber size in fast muscles compared to wild type mice (Hughes *et al.*, 1999). However, no effect on MyHC composition was observed. These results were also observed when myogenin DNA was electroporated into muscles of adult mice (Ekmark *et al.*, 2003).

Other pathways have been shown to alter MyHC composition in a slow oxidative direction, and special attention has been paid to calcium-triggered regulatory pathways acting through calcineurin (CaN) and Ca^{2+}-calmodulin-dependent protein kinase (CaMK) (figure 1.1)

(Koulmann & Bigard, 2006). CaN is a serine-threonine Ca^{2+}/Calmodulin (CaM)-regulated protein phosphatase that acts on the transcription factor nuclear factor of activated T cells (NFAT) family, inducing their translocation to the nucleus and binding to promoter regions of different target genes (Rao *et al.*, 1997). CaN is a heterodimer which consists of a catalytic (CnA) and a regulatory (CnB) subunit. Both the CaN subunits and NFAT have various isoforms, and skeletal muscles express CnB1, CnAα and CnAβ, as well as NFATc1-c4 (Schiaffino *et al.*, 2007). Calabria *et al.* (2009) have suggested that the transcription of slow and fast MyHC genes uses different combinations of the 4 NFAT isoforms (NFATc1-c4). CaN is thought to contribute to transition of MyHC isoform expression in a fast-to-slow direction, both *in vitro* and *in vivo*, through the activation of NFAT (Chin *et al.*, 1998; Dunn *et al.*, 1999; Bigard *et al.*, 2000; Rana *et al.*, 2008). The transactivational activity of NFAT on slow gene programs (McKinsey *et al.*, 2002) is known to require interactions with other transcription factors, such as myocyte enhancer factor (MEF)-2 (Wu *et al.*, 2000). MEF-2 interacts with, and mediates, a large set of reactions and is activated through the CaMK pathway (McKinsey *et al.*, 2000). The rate of transcription is often dramatically increased after MEF-2 phosphorylation on its transcriptional activation domain (on the C-terminal end) by the p38 mitogen-activated protein kinase (MAPK) (Zhao *et al.*, 1999; McGee & Hargreaves, 2004). However, MEF-2-mediated transcription is dependent upon dimerization and association with different cofactors possessing histone acetyltransferase (HAT) activity (McKinsey *et al.*, 2002). Both NFAT (McKinsey *et al.*, 2002) and peroxisome proliferator-activated receptor (PPAR) gamma coactivator (PGC)-1α (Scarpulla, 2002) have the ability to recruit coactivators with HAT activity, such as steroid receptor coactivator (SRC)-1 and CREB binding protein (CBP)/p300 (Puigserver *et al.*, 1999), to transcription factors, thereby activating transcription by histone acetylation.

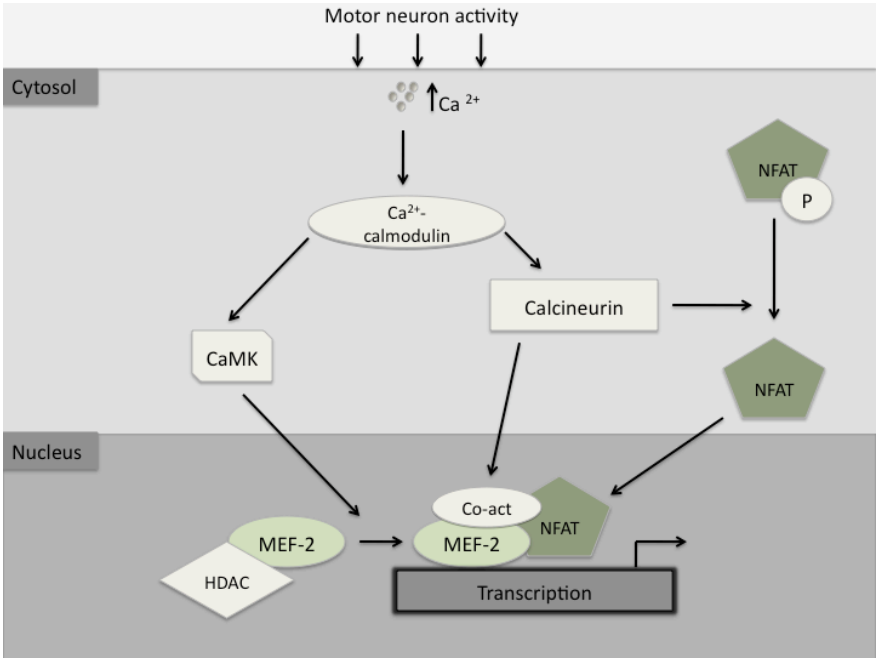

Figure 1.1 Signaling pathway through the calcinurin (CaN) and Ca^{2+}-calmodulin-dependent protein kinase (CaMK)

Schematic diagram summarizing CaN signaling through its two major downstream substrates, the nuclear factor of activated T cells (NFAT) and the myocyte enhancer factor (MEF)-2. Different co-activators (Co-act) with the ability to recruit proteins with histone acetyltransferase (HAT) activity are recruited to the transcription site to aid the expression of genes meditated by these pathways. Histone deacetylase (HDAC) is phosphorylated by CaMK, and thus contributes to the activation of the MEF2 transcription factor by releasing it from HDAC. The figure is adapted from Koulmann & Bigard (2006).

The fatty acid activated transcription factors PPARs are nuclear receptors, which have been found to play master regulatory roles in development, inflammation, glucose and lipid metabolism (Schmidt *et al.*, 1992; Xu *et al.*, 1999; Willson *et al.*, 2000; Blaschke *et al.*, 2006). Three mammalian subtypes, all closely related and encoded by separate genes, have been identified: α, ɣ, β/δ (Dreyer *et al.*, 1992; Kliewer *et al.*, 1994). PPARα has the ability to induce transcription of genes involved in mitochondrial fatty acid oxidative pathway through the activation of PGC-1α. PPARβ/δ has been shown to regulate, in addition to β- and ω-oxidation of fatty acids (Oliver *et al.*, 2001; Wang *et al.*, 2003), expression of mitochondrial DNA (mtDNA) and slow contractile protein genes. This results in an increased resistance to fatigue and a more oxidative fiber type profile (Luquet *et al.*, 2003; Wang *et al.*, 2004) also in adult mice (Lunde *et al.*, 2007). PPARɣ has been found to be a master regulator of adipogenesis (Tontonoz *et al.*, 1994a; Tontonoz *et al.*, 1994b; Rosen & Spiegelman, 2000), and

is predominantly expressed in white adipose tissue and brown adipose tissue, as well as in macrophages, colon and placenta (Braissant *et al.*, 1996).

PGC-1α was originally identified as a coactivator for PPARγ when induced by cold exposure in brown adipose tissue (Puigserver *et al.*, 1998). However, PGC-1α has later been shown to interact with a myriad of other transcription factors both inside and outside the nuclear receptor family in a ligand-dependent or -independent fashion (Lin *et al.*, 2005). This makes PGC-1α highly versatile and capable of activating distinct biological programs in different tissues. PGC-1α is particularly expressed in oxidative tissues, such as heart, brain, kidney, liver, white and brown adipose tissue and skeletal muscle (Puigserver *et al.*, 1998). Different pathways, such as p38 MAPK (Akimoto *et al.*, 2005), CaMK and CaN (Handschin *et al.*, 2003), have been shown to regulate and control PGC-1α expression (figure 1.2) (Koulmann & Bigard, 2006). PGC-1α controls adaptive thermogenesis through the up-regulation of uncoupling protein (UPC)-1 in brown adipose tissue, but also in skeletal muscle (Puigserver *et al.*, 1998). In addition, PGC-1α has been shown to interact with UPC-1 during brown adipocyte differentiation (Lin *et al.*, 2002a). PGC-1α has also been shown to stimulate mitochondrial biogenesis and oxidative enzymes in different cell types by inducing the expression of the estrogen related receptor (ERR)-α and the nuclear respiratory factors (NRF)-1 and 2, and by co-activating the transcriptional activity of NRF-1 (Wu *et al.*, 1999; Mootha *et al.*, 2004; Schiaffino *et al.*, 2007). NRF-1 and 2 are in turn able to stimulate the expression of genes primarily involved in oxidative phosphorylation and mtDNA transcription and replication (Scarpulla, 2002). PGC-1α has also been shown to increase mitochondrial biogenesis *in vivo* (Lehman *et al.*, 2000). As mentioned above, PGC-1α has the ability to induce MEF-2-mediated transcription through its ability to recruit HATs (McGee & Hargreaves, 2004). Interestingly, knockout mice or mice targeted with a disrupted PGC-1α gene are viable and show only mild mitochondrial impairments (Scarpulla, 2006).

The importance of PGC-1α in the control of oxidative metabolism, as previously mentioned, an important factor in fiber type diversity, resulted in the interest in PGC-1α's effect on fiber type switching. PGC-1α is preferentially expressed in slow muscles (Lin *et al.*, 2002b), and in denervated muscles the expression of PGC-1α decreases (Koves *et al.*, 2005). However, exercise in both rodents and humans readily induces PGC-1α expression, possibly through the p38

MAPK pathway (figure 1.2) (Schiaffino *et al.*, 2007). Phosphorylation of PGC-1α by p38 MAPK leads to nuclear translocation of PGC-1α and increased expression of mitochondrial enzymes (Wright *et al.*, 2007). Overexpression of PGC-1α in skeletal muscle of transgenic mice induced slow-type-1 and 2a fibers in fast glycolytic muscles, in addition to stimulating the mitochondrial biogenesis and synthesis of oxidative enzymes; thus making the muscles more resistance to fatigue (Lin *et al.*, 2002b). In PGC-1α knockout mice the number of these fibers appear normal, indicating that PGC-1α clearly not is the sole determinant for type 1 and 2a fibers (Arany *et al.*, 2005).

In addition to regulating mitochondrial biogenesis, oxidative enzymes, and a slow MyHC gene program, PGC-1α also has the ability to up-regulate genes of the mitochondrial fatty acid oxidative pathway in skeletal muscles through the activation of PPARα (figure 1.2) (Vega *et al.*, 2000; Lee *et al.*, 2006). GLUT4 expression is known to be enhanced by PGC-1α via coactivation of MEF-2 in skeletal muscles (Michael *et al.*, 2001).

Recent data indicate that the later-identified homologue to PGC-1α, PGC-1β, may also be involved in the activation of mitochondrial biogenesis and muscle plasticity through some of the same pathways as PGC-1α (Lin *et al.*, 2002a; Lin *et al.*, 2005; Mortensen *et al.*, 2006; Arany *et al.*, 2007).

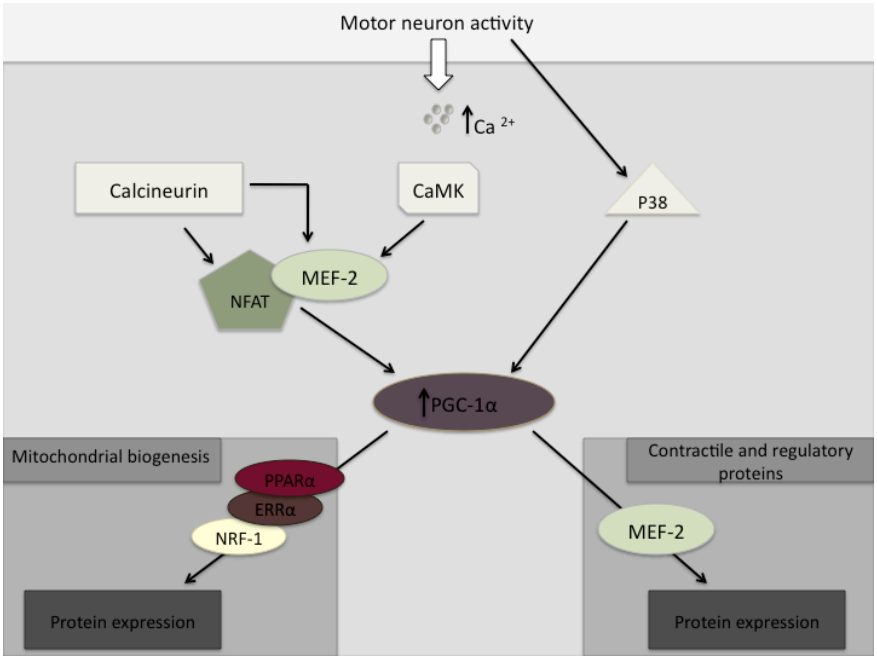

Figure 1.2 Activation of PPAR-gamma-coactivator (PGC)-1α and some of the downstream regulation involved in mitochondrial biogenesis and fiber type switching

Ca^{2+}/calmodulin-dependent protein kinase (CaMK), myocyte enhancer factor (MEF)-2 and calcineurin, together with p38, play distinct but overlapping roles in increasing PGC-1α expression. In combination with nuclear factor of activated t-cells (NFAT), activated-MEF-2 can bind coactivator proteins such as PGC-1α. Through binding of nuclear respiratory factor (NRF)-1, estrogen related receptor (ERR)α, and peroxisome proliferation-activated receptor (PPAR)α, PGC-1α has the ability to coordinate expression of genes involved in mitochondrial biogenesis and oxidative phosphorylation, as well as, contractile and regulatory proteins in muscles. This figure is adapted from Koulmann & Bigard (2006).

1.4 PPAR-gamma coactivator-1β (PGC-1β)

The PGC-1 family of coactivators consists of PGC-1α, PGC-1β and the PGC-1 related coactivators (PRC). This family is highly conserved between many chordate species, such as humans, primates, rodents, ruminants, birds, amphibians, and fish (Lin *et al.*, 2005), suggesting an important role common to all of these species (Lin *et al.*, 2002a). Lin *et al.* (2002a) and Kressler *et al.* (2002) found a close homologue to PGC-1α, named PGC-1β, through searches of new data base entries. This 3.6 kb mouse complimentary DNA (cDNA) has an open reading frame of 1014 amino acids, which corresponds to a molecular size of 112.1 kDa. Unlike the PGC-1 related coactivators (PRC) (Andersson & Scarpulla, 2001), sequence similarity between PGC-1α and -1β is distributed along the entire length of the protein with greater identity in the N-terminal activation domain (AD) and the C-terminal RNA

recognition motif (RRM), 40 and 48 %, respectively (figure 1.3) (Lin *et al.*, 2002a). Even though these are all closely related homologues expressed primarily in the same tissues, they have distinct and often opposite biological activities.

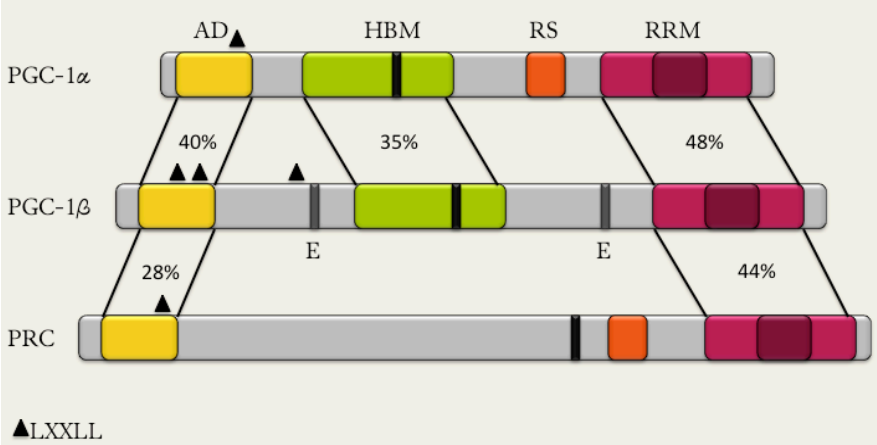

Figure 1.3 Protein sequence alignment of PGC-1β, PGC-1α and PRC.

Protein sequence alignment of the PGC-1 family of coactivators; with the degree of sequence similarity to PGC-1β shown. Conserved domains/motifs are indicated above the diagram, and includes the activation domain (AD), host cell factor (HCF) binding motif (HBM), RNA recognition motif (RRM), arginine/serine-rich motif (RS) and leucine-rich domains (LXXLL). PGC-1β also contains two glutamic/aspartic acid-rich domains (E), in contrast to PGC-1α and PRC, which has an arginine/serine-rich motif (RS). Figure is not drawn to scale, and is based on Lin *et al.* (2002a)

The tissue distribution of PGC-1β mRNA corresponds to that of PGC-1α, with the highest levels in brown adipose tissue and heart (Lin *et al.*, 2002a; Scarpulla, 2002), but it is also found in other oxidative tissues, such as brain, liver, white adipose tissue, and muscle (Puigserver *et al.*, 1998; Lin *et al.*, 2002a; Kamei *et al.*, 2003). However in brown adipose tissue, PGC-1β is not induced by cold exposure as PGC-1α (Lin *et al.*, 2002a). In contrast to PGC-1α, PGC-1β does not work through the activation of the UCP-1 promoter and does not have the ability to stimulate PPARγ-mediated transcription (Kamei *et al.*, 2003).

Despite the differences between PGC-1β and -1α, PGC-1β binds NRF-1 and ERRα, and transactivates their target genes leading to increased mitochondrial gene expression, by the same mechanisms as PGC-1α (Kamei *et al.*, 2003; Lin *et al.*, 2003). PGC-1β has also been shown to be equally potent as PGC-1α to activate a full program of mitochondrial biogenesis and oxidative enzymes in isolated cells (St-Pierre *et al.*, 2003) and *in vivo* (Arany *et al.*, 2007). However, PGC-1α has been associated with higher proton leak rates than PGC-1β (St-Pierre

et al., 2003). Since the tissue-specific expression pattern of the two coactivators is very similar, PGC-1β may compensate for the absence of PGC-1α in PGC-1α knockout mice by maintaining the mitochondrial functions (Scarpulla, 2006).

1.5 PGC-1β and skeletal muscle

During the last few years, knowledge about the physiological functions of PGC-1β in skeletal muscle has increased considerably. Strong evidence suggests that PGC-1β is an important regulator of mitochondrial biogenesis and oxidative enzymes, such as its homologue PGC-1α (St-Pierre *et al.*, 2003; Arany *et al.*, 2007). In skeletal muscle, one of the most oxidative tissues in the body, PGC-1β is highly expressed (Lin *et al.*, 2002a). PGC-1β knockout mice have reduced expression of oxidative phosphorylation genes and mitochondrial dysfunction in skeletal muscles (Vianna *et al.*, 2006). PGC-1β, as PGC-1α, has been shown to be a potent enhancer for GLUT4 expression via MEF-2 in cultured skeletal muscle myotubes from rat (Mortensen *et al.*, 2006).

In addition to activating a full program of mitochondrial biogenesis and oxidative enzymes, PGC-1β has been shown to induce fiber type switching in transgenic mice partly via coactivation of the MEF-2 transcription factor (Arany *et al.*, 2007). PGC-1β's influence on fiber type maturation was shown by Mortensen *et al.* (2006) when they overexpressed PGC-1β by adenovirus-mediated gene transfer in cultured neonatal myoblasts, primarily from rat skeletal muscle. Both PGC-1β and -1α seem to be involved in maturation of myofibers by downregulating $MyHC_{emb}$ (embryonic) and $MyHC_{peri}$ (perinatal).

Arany *et al.* (2007) further explored the functions of PGC-1β by transgenic expression of this protein in skeletal muscle. Remarkably, this transgenic overexpression of PGC-1β induced a significant increase in the amount of MyHC 2x mRNA, in expense of MyHC 1, 2a and 2b, compared to wild type littermates. The induction of mitochondrial biogenesis and gene expression of the 2x MyHC isoform resulted in transgenic animals capable of withstanding more work over time than wild type animals. These transgenic mice were able to run, on an average, for 32.5 min to exhaustion, compared to 26 min for the control mice, which reflects a distance run of 746 meters, versus 516 meters, respectively. Interestingly, transgenic expression

of PGC-1β in all tissues at once leads to resistance to diabetes and hypermetabolism (Kamei *et al.*, 2003).

Because PGC-1β has been shown to interact in myofiber maturation (Mortensen *et al.*, 2006), the results in transgenic mice presented by Arany *et al.* (2007) cannot be ruled out as PGC-1β's role in myogenesis, rather than true adult plasticity. One of the aims for this thesis was therefore to investigate PGC-1β's effect on MyHC expression in adult mice, where myogenesis no longer is an involving factor.

Furthermore, Arany *et al.* (2007) investigated the mRNA level of endogenous PGC-1β in homogenates from different wild type mice muscles, and compared it to the mRNA level of all MyHC isoforms. A good correlation between the mRNA expression of PGC-1β and the MyHC 2x isoform was seen in all muscles examined, with the exception of SOL. PGC-1β mRNA expression was found to be high in SOL, although higher in the fast EDL. These results support the hypothesis of a role for PGC-1β in the regulation of 2x fibers. However, the subcellular localization and the relative protein level of PGC-1β in SOL and EDL has not yet been investigated, and was therefore one of the aims of this study.

Taken into account these *in vitro* and *in vivo* observations, PGC-1β is implicated as a potent regulator of mitochondrial biogenesis and a key molecular switch in the regulation of muscle fiber phenotype.

In this master thesis, overexpression of the PGC-1β protein in individual skeletal muscle fibers of mice was investigated in context of the underlying mechanisms that determine adult fiber phenotype plasticity, and in this way, developmental effects were precluded.

1.6 Aims

1. **What is the expression pattern of PGC-1β protein within wild type fast and slow muscles?**

   To address this question, EDL and SOL muscles from wild type mice were homogenized, and protein was extracted and fractionated into nuclear and cytosolic samples. Western blots were performed and PGC-1β was visualized by antibody staining.

2. **Will PGC-1β overexpression in adult mice induce phenotypic changes in individual skeletal muscle fibers?**

   To answer this, Flag-PGC-1β was transfected into muscle fibers of both EDL and SOL of adult mice by *in vivo* electroporation. MyHC expression of the transfected fibers was analyzed fourteen days after transfection and compared to sham-transfected and normal non-transfected control fibers.

2. MATERIALS AND METHODS

2.1 DNA Constructs

For overexpression of PGC-1β, a 9.1 kb plasmid, pcDNA-f:PGC-1β, (1031, Addgene) (figure 2.1A) encoding a constitutively active Flag-PGC-1β fusion protein was bought from Addgene (1031). DNA sequence encoding the Flag-tag had been fused N-terminally to the PGC-1β gene and the transgene is driven by the constitutively active cytomegalovirus (CMV) promoter.

Serving as sham control, a modified pcDNA-f:PGC1β plasmid was prepared (figure 2.1B). The DNA sequence encoding PGC-1β was cut out using the restriction enzyme EcoRI. Following restriction cutting, the plasmid was religated using T_4 ligase and transformed into CaCl competent *Escherichia coli (E.coli)* cells. The amplified plasmid was then extracted from the bacteria by a miniprep DNA purification system. For verification, restriction cutting with HindIII and sequencing using a T7 primer was performed. This resulted in a sham plasmid with the flag-tag, but without the PGC-1β gene, that we designated pcDNA-f.

In addition, a reporter plasmid, pAP-lacZ (figure 2.1C), was used. The 7.8 kb pAP-lacZ plasmid contains the *E.coli* β-galactosidase sequence which is driven by a rous sarcoma virus (RSV) promoter and an origin of replication driven by a simian virus (SV) 40 promoter. This plasmid was a kind gift from Professor N. Gautam.

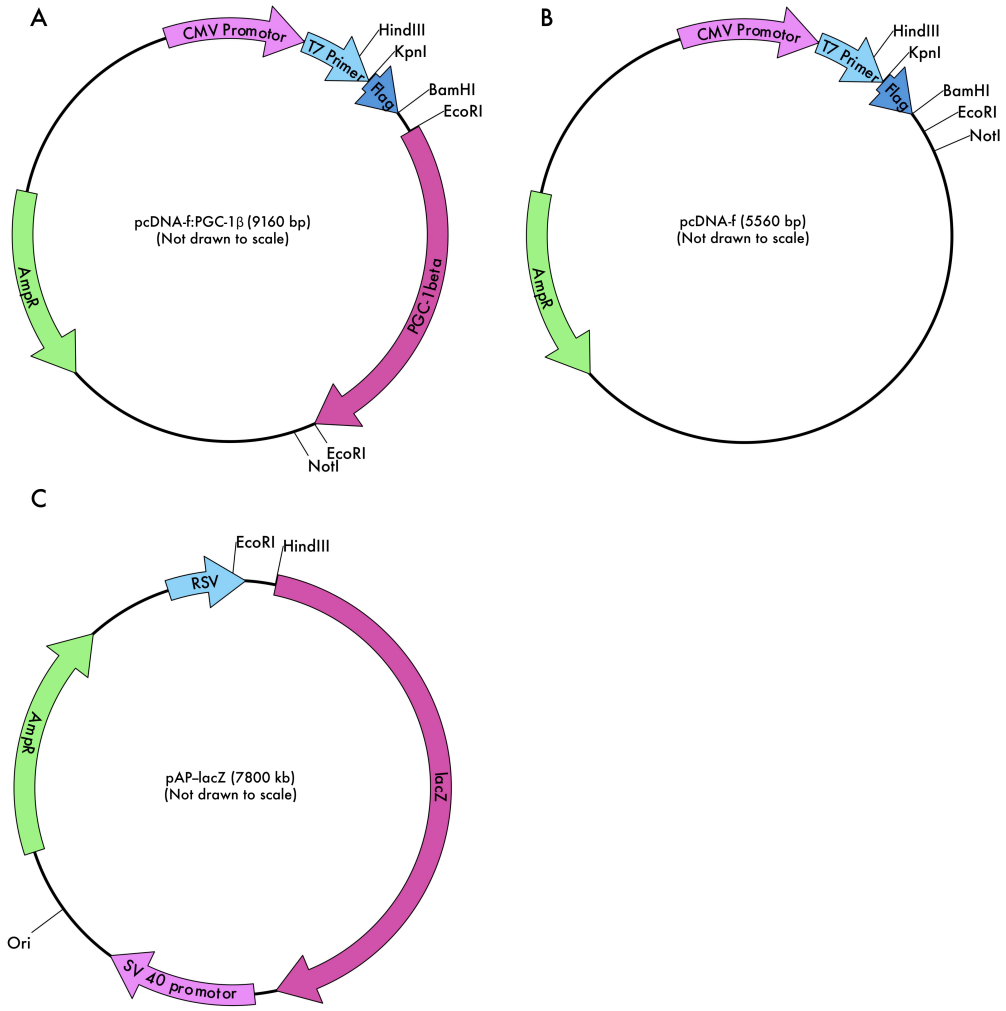

Figure 2.1 Expression vectors.

A. The 9.1 kb pcDNA-f:PGC-1β plasmid, encoding the fusion protein Flag-PGC-1β **B.** The 5.6 kb pcDNA-f sham plasmid, encoding the flag-tag. **C.** The 7.8 kb reporter plasmid, pAP-lacZ, encoding β-galactosidase.

2.2 Animals

Female NMRI mice (20-25 g), delivered by Scanbur (BK), were used for this study. They were held in cages in the animal research facility at the Department of Molecular Biosciences, University of Oslo. The air temperature and humidity were kept at 21-24 °C and 50-60 %, respectively. The light was regulated at 12- h cycles. Food and water was given *ad libitum*.

All animal experiments were conducted according to the Norwegian Animal Welfare Act of December 20th, 1974, no. 37, chapter VI, sections 20-22, and the Regulation on Animal

Experimentation of January 15th, 1996, as well as reviewed and approved by the Norwegian Animal Research Authority.

2.3 Surgery

2.3.1 Anesthesia

Each animal was initially anesthetized with 1.9-2.5 % v/v of Isoflurane gas (506949, Florene, Abbot) with airflow of 500-600 cc/min, or an intraperitoneal injection of 5 μl/g body weight Equithesin for the electroporation and termination experiments, respectively. By pinching the metatarsus region and observing the absence of the withdrawal reflex, the effect of anesthesia was regularly checked. Further anesthesia was administrated if necessary.

2.3.2 Surgical procedures

When deep anesthesia was induced, hair was removed from the lower part of the leg by an electric shaver and hair removal cream (Veet, Reckitt and Coleman). The leg was locked in a fixed position onto a platform and the muscle surgically exposed. For transfection of muscle fibers, the DNA solution (appendix A, 5.1.1, 5.1.2) was injected into the belly of the muscle, followed by electroporation. The wound was covered at all times in ringer acetate solution (Fresenius Kabi Norway AS) to prevent dehydration of the muscle. After electroporation, surgical sutures were used to close the wound.

After fourteen days the animals were re-anesthetized; this time by intraperitoneal injections of Equithesin (704845, Ullevål sykehusapotek, Norway). The muscle was surgically exposed and excised. While still under deep anesthesia, the animal was sacrificed by neck dislocating. The excision of wild type muscles was performed in the same way.

2.3.3 Freezing of muscles

After excision the muscles were slightly stretched between two pins in a homemade form and embedded in Tissue-Tek (4583, Sakura Finetek). It was further frozen in isopentane (24872.323, GPR Rectapur), which was cooled down to its freezing point (-160 °C) by liquid nitrogen (-196 °C), and stored in 2 ml microtubes (72.694.006, Sarstedt) at -80 °C until used for histochemical analyses.

Muscles intended for homogenization and fractionation were frozen directly in liquid nitrogen and stored in 2 ml microtubes (72.694.006, Sarstedt) at -80 °C.

2.4 Transfection of plasmids

2.4.1 Transfection in tissue culture

To verify the translation of the Flag-PGC-1β transgene into a fully functional protein, human embryonic kidney cells (HEK 293) were transfected, and the protein lysate was visualized on Western blots.

The HEK 293 cells were cultured at 37 °C in an atmosphere of 5 % CO_2 in Dulbecco's modified Eagle's medium (DMEM) (41966-029, GIBCO) with 5 % fetal calf serum (FCS) (14-416F, Bio Whittaker) and 100 U/ml Pen/Strep (DE17-602E, Bio Whittaker), an antibiotic solution containing both penicillin and streptomycin (appendix 5.2.1). The cells were split 1:6 every fourth day with trypsin ethylenediaminetetraacetic (EDTA) (BE17-161E, Bio Whittaker).

Transfection with the expression plasmids pcDNA-f:PGC-1β was carried out according to the Lipofectamine 2000 kit (11668019, Invitrogen). As sham control, cells were transfected with the vector pcDNA-f, while non-transfected cells were used as a negative control.

2.4.2 *In vivo* electroporation

In vivo electroporation has previously been described by Mathiesen (1999), and is a mechanism for inducing uptake of foreign DNA into a cell**.** Electroporation is based on the principle that each cell has a given transmembrane threshold, and the electric field applied has to excide this threshold for the cells to get permeabilized (Rols & Teissie, 1990; Golzio *et al.*, 2001, 2002; Rols, 2006). This critical threshold is dependent upon the cell size, increasing with decreasing size (Rols, 2006).

Following surgical exposure of the muscles, 10 μl of 0.5 μg/μl DNA solution (appendix 5.1.1, 5.1.2) was injected into the muscle fibers using a U-100 insulin BD Micro-Fine ™ syringe. Immediately following the injection, the muscle was subjected to five trains (with 1s intermission between each train) of 1000 symmetrical bipolar electrical pulses (200 μs in each directions) with a peak-to-peak voltage of 20 V. This was delivered by means of a pair of 1 mm thick/2 cm long silver electrodes, one on each side of the muscle, approximately 3-5 mm apart.

The electrical field was created by a pulse generator, (Pulsar 6bp-a/s, Fredrick Haer and Co), and the electrical charge was registered with an analogue oscilloscope (03245A, Gould Advance).

10 μl of DNA solution containing a mix of the expression plasmid pcDNA-f:PGC-1β and the reporter plasmid pAP-lacZ (appendix A, 5.1.1) was injected into the right leg of both EDL and SOL. A similar DNA solution containing the sham plasmid, pcDNA-f and pAP-lacZ was injected into the left leg (appendix A, 5.1.2). This resulted in two different experimental groups from the right and left leg; with the pcDNA-f:PGC-1β transfected fibers as one and the pcDNA-f transfected fibers as the other. These two groups are from now on referred to as PGC-1β-transfected fibers and sham-transfected fibers, respectively.

In addition another group, which served as an internal control, was made up of a large number of randomly selected non-transfected fibers (hereafter called the normal control fibers). Because of an earlier reported "sham effect" (normal control and sham-transfected fibers differed significantly) with mice in our group, normal control fibers were picked in two different ways to ensure an unbiased material. Fibers were either selected as the nearest fiber down to the left (or up to the right depending on what was possible) from the transfected fibers (PGC-1β transfected fibers), or a large number of fibers surrounding each transfected fiber (sham transfected fibers). The normal control fiber type distribution from the PGC-1β-transfected and the sham-transfected fibers did not differ significantly, and are presented as on group. This strongly indicates that the sham effect is not due to how the normal fibers were picked, but rather some unknown effect of overexpression or the method of electroporation in mice.

The three groups described above (table 2.1) consist of pooled data from several animals, as no systematic inter-animal variations were observed.

Table 2.1 Overview of experimental groups, expression vectors and overexpressed proteins

Groups:	Expression vectors:	Overexpressed proteins:
Control fibers	-	-
Sham transfected fibers	pcDNA-f pAP-lacZ	Flag β-galactosidase
PGC-1β transfected fibers	pcDNA-f:PGC-1β pAP-lacZ	Flag-PGC-1β β-galactosidase

Three groups, two experimental and one internal control, with the following expression vectors injected and electroporated, and the respective overexpressed protein. Expression vector pcDNA-f:PGC-1β/pAP-lacZ was injected in the right leg (PGC-1β-transfected fibers), while the pcDNA-f/pAP-lacZ was injected into the left (sham-transfected fibers). Normal control fibers are represented from both legs and pooled together.

2.5 Protein extraction and measurement

2.5.1 Whole cell protein extraction from cell culture

48 h after transfection of the HEK 293 cells, medium was removed, cells put on ice and washed twice in ice-cold phosphate buffered saline (PBS) (20012-043, GIBCO). The cells were further lysed in 500 µl lysis buffer (Cameron *et al.*, 2008) (appendix 5.2.2) and centrifuged for 20 min at 13 000 g at 4 °C. The supernatant was stored at -80 °C.

2.5.2 Fractionation of protein from wild type muscles

To evaluate expression of the endogenous PGC-1β protein in wild type SOL and EDL, the muscles were homogenized, fractionated and run on a Western blot. 12 normal (6 mice), untreated muscles of the same type (SOL or EDL) were pooled together and crushed with a mortar and pestle before being transferred to a falcon tube. Electrical homogenization (IKA Labortechnik T25 basic, Tamiro Lab AS) was carried out to ensure thorough crushing. The cytoplasmic and nuclear protein fractionation was performed according to the Compartmental protein extraction kit (2154, Chemicon International). To determine the protein concentration the Bio-Rad protein assay system was used according to the protocol (500-0006, Bio-Rad) and read at 595 nm by a microplate reader (Wallac Victor^2 1420, Perkin Elmer). The samples were further aliquoted and stored at -80 °C.

2.6 SDS-PAGE and Western Blotting

Sodium dodecyl sulphate polyacrylamide gel (SDS-PAGE) and Western blotting was performed according to the NuPAGE Technical Guide (IM-1001, Invitrogen Instruction Manual (2003)). The electrophoresis was run at 200 V for 90 min using MOPS as a running buffer (NP0001, Invitrogen). 40 µg of protein extract, from both transfected HEK 293 cells and normal muscles from female NMRI mice, was run on NuPAGE® Novex 4-12% Bis- Tris Gels (NP0321BOX, Invitrogen). Both Sharp Pre-stained protein ladder (LC5800, Invitrogen) and SeeBlue plus2 Pre-stained protein ladder (LC 5925, Invitrogen) were used.

Blotting was performed at 30 V for 90 min (as described in XCell II Blot Module, IM-9051, Invitrogen Instruction Manual 2003). Membranes were blocked in 5 % dry milk (7352F, Acumedia) in tris-buffered saline with tween20 (TBS-T) (appendix 5.3.1) at 4 °C overnight. Primary antibodies were diluted in 5 % dry milk and secondary antibodies in 1.3 % dry milk.

Visualization of transgenic (from cell lysate) and endogenous PGC-1β protein (from muscle extract) was achieved by application of a rabbit polyclonal anti-flag primary antibody (1:300, F7425, SIGMA) and a rabbit polyclonal anti-PGC1β antibody (1:1000, NB110-58858, Novus Biologicals), respectively, followed by goat horse-radish peroxidase (HRP) conjugated anti-rabbit immunoglobulin (Ig)G secondary antibody (1:1750, 4030-05, SouthernBiotech). Immunostaining was followed by visualization on film (28906837, Amersham) using the ECL Western Blotting Detection kit (RPN2109, Amersham).

Even loading, in whole cell lysate, was controlled by the application of a mouse monoclonal anti-actin IgG antibody (1:500, Sc-8432, Santa Cruz Biotechnology), followed by a sheep HRP conjugated anti-mouse IgG secondary antibody (1:1750, NA931VS, Amersham). The purity of the subcellular protein fractions was controlled by the application of goat polyclonal anti-GAPDH antibody (1:500, Sc-20357, Santa Cruz Biotechnology) and rabbit polyclonal anti-Oct-4 antibody (1:1000, 3576-100, Biovision), followed by rabbit HRP conjugated anti-goat IgG secondary antibody (1:1750, 6160-05, SouthernBiotech) and goat HRP conjugated anti-rabbit IgG secondary antibody (1:1750, 4030-05, SouthernBiotech), respectively. Octamer (Oct)-4 transcription factor was used as a nuclear marker, whereas glyceraldehyde 3-phosphate

dehydrogenase (GAPDH) was used as a cytosolic marker. The expression of GAPDH should be higher in the glycolytic EDL than in the oxidative SOL muscle (Okumura *et al.*, 2005).

To measure the relative amount of protein, Western blot bands were quantified using ImageJ (NIH).

2.7 Histochemistry

2.7.1 Preparation of transverse muscle serial sections

The frozen muscles were cryosectioned at 10 μm using a cryostat (HM560M Microme). The temperature of the muscle tissue was set to -26 °C and the knife to -24 °C. Transverse serial sections were mounted on SuperFrost Plus slides (J1800AMNZ, Menzel-Gläser) and stored at -80 °C until further histochemical analyses.

2.7.2 Staining for β-galactosidase activity

As previously mentioned, the pAP-lacZ plasmid was co-transfected along with the experimental plasmid, pcDNA-f:PGC1-β and the sham plasmid, pcDNA-f, as a reporter gene for identification of the transfected fibers (Lojda, 1970; Sanes *et al.*, 1986). pAP-lacZ encodes the β-galactosidase enzyme for which the activity can be visualized histochemically in a color reaction (appendix 5.4.2). When adding the enzyme's substrate, 5-bromo-4-chloro-3-indolyle-β-D-galactoside (X-gal) to the colorless product indoxyle, the indoxyle dimerises and makes insoluble blue crystals that can be visualized under the microscope (figure 2.2). Since co-transfection of two separate plasmids into muscle fibers by *in vivo* electroporation results in nearly 100 % co-expression, the stained fibers are also likely to express the protein of the other plasmid (Rana *et al.*, 2004)

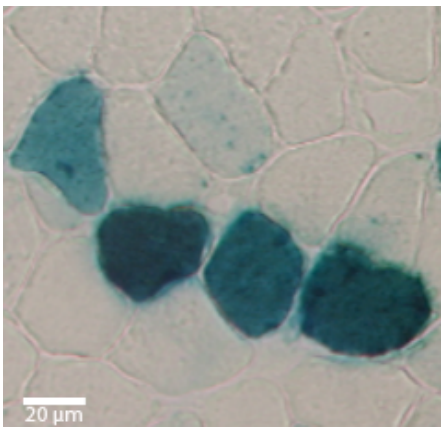

Figure 2.2 β-galactosidase staining

β-galactosidase staining on a cross section of *soleus*. The blue fibers are identified as the lacZ transfected fibers, in contrast to the non-transfected colorless ones. Scale bar: 20 μm

2.7.3 Staining for myosin heavy chain isoforms and laminin

To determine the muscle fiber types, monoclonal antibodies against the four main MyHC subtypes were used on neighboring sections. These antibodies were kindly provided by Stefano Schiaffino's lab. A specific antibody against the 2x MyHC isoform (6H1) was a kind gift from Joseph F.Y.Hoh, but in this case it stained poorly, and therefore was not further used. The suitable secondary antibodies (table 2.2, appendix 5.4.3) were conjugated to fluorescent dyes such as cyanine (Cy-3) and fluroscein (FITC). When Cy-3 or FITC is illuminated with green (λ=546 nm) or blue-green (λ=485 nm) light, respectively, fluorescence is emitted and the positive fibers will light up, while the negative ones will remain dark (figure 2.3).

Laminin is a major protein of the basal laminia, a protein network in the extracellular matrix surrounding the cell membrane. By staining sections with a rabbit anti-laminin primary antibody (1:600, L9393, Sigma), followed by a goat isothiocyanate (TRITC) conjugated anti-rabbit IgG secondary antibody (1:200, T6778, Sigma) (appendix 5.4.3) and illuminated the muscle sections with green light (λ=546 nm), the contour of the individual cell can be visualized and easily distinguished from each other. This makes MyHC-fiber typing less difficult to perform.

An example of a histochemical analysis on serial sections from EDL is shown in figure 2.3, comparing β-galactosidase and anti-MyHC staining on a PGC-1β-transfected muscle section. Randomly selected non-transfected fibers are marked N1-6, while β-galactosidase positive staining are marked P1-6. Laminin staining is also shown.

Table 2.2 Overview of antibodies used to identify MyHC subtype expression in muscle fibers

MyHC:	Primary antibody:	Secondary antibody:
1	BA-D5	Rabbit anti-mouse IgG, FITC conjugated (F-9137, SIGMA)
2a	SC-71	Rabbit anti-mouse IgG, FITC conjugated (F-9137, SIGMA)
All non-2x	BF-35	Rabbit anti-mouse IgG, FITC conjugated (F-9137, SIGMA)
2b	BF-F3	Goat anti-mouse IgM, Cy-3 (J115-165-020, Jackson ImmunoReasearch Lab)

An overview of the primary and secondary antibodies used to identify the different subtypes of MyHC in the individual muscle fibers of transfected *soleus* and *extensor digitorum longus*.

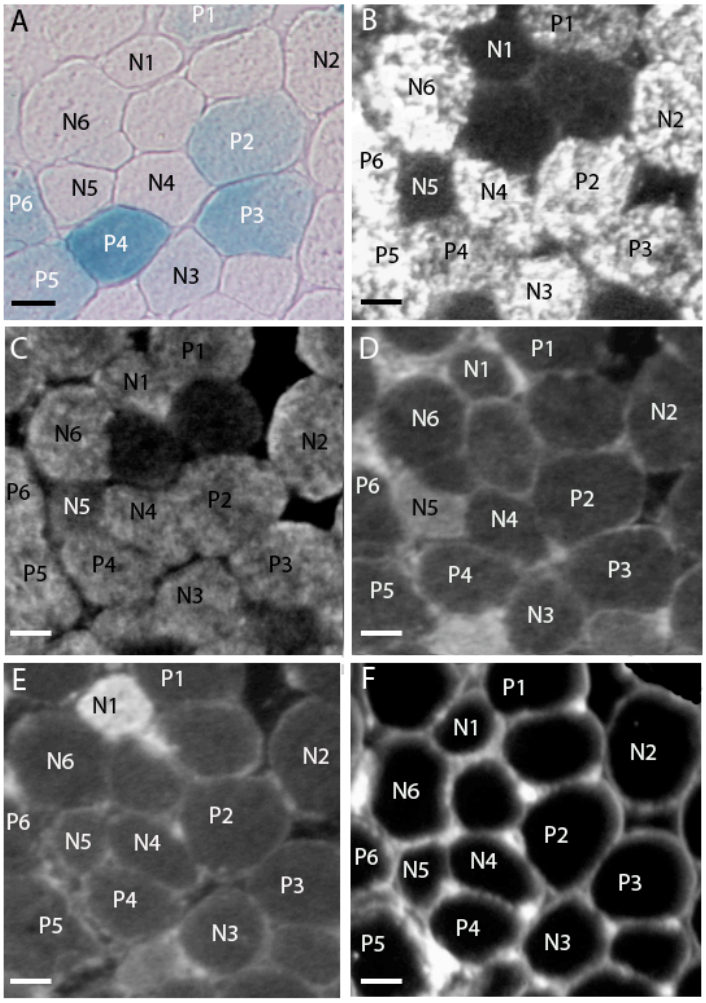

Figure 2.3 A-F Example of serial sections stained with β-galactosidase, anti-myosin heavy chain (MyHC) and anti-laminin in a PGC-1β transfected EDL muscle

Serial cross sections stained for β-galactosidase activity (**A**), MyHC 2b (**B**), non-MyHC 2x (**C**), MyHC 2a (**D**), MyHC 1 (**E**) and laminin (**F**). **A.** Positively stained β-galactosidase fibers appear blue (P1-6), while randomly selected non-transfected control fibers are β-galactosidase negative, and appear bright (N1-6). **B-E.** Positively stained fibers appear bright for their respective MyHC isoform, while the dark fibers represent negatively stained fibers with a different MyHC isoform. **F.** Anti-laminin staining shows the cell membrane of each fiber. Scale bare A-F: 20 μm

In addition to the four main fiber type populations, which contain only a single MyHC isoform (Reiser *et al.*, 1985; Schiaffino *et al.*, 1989), some fibers stained positive for two or more subtypes of MyHC. The population of intermediate hybrid fibers includes 1/2a, 2a/2x and 2x/2b (Pette & Staron, 1993; Schiaffino & Reggiani, 1994), and during some experimental conditions aberrant hybrid fibers such as 1/2b, 1/2a/2b and 1/2x/2b has also been documented (Caiozzo *et al.*, 1998). However, since the specific 2x antibody (6H1) worked poorly in mice this made it impossible to determine 2a/2x and 2x/2b hybrids, the most important hybrids in this thesis.

2.8 Imaging

2.8.1 Bright-field imaging

Images from muscle cross sections stained for β-galactosidase activity were taken with a color-chilled 3CCD video camera (C5810, Hamamatsu) connected to a microscope (BX50WI, Olympus). The images were taken with a 10X water immersion objective (UMFPlanF1, Olympus), the images were further digitalized through an image-processing unit (Argus 20,

Hamamatsu), and transferred to a Power Macintosh G3 computer. The processing of the material was carried out using Adobe Photoshop CS3.

2.8.2 Fluorescence imaging

Muscle cross sections stained with Cy-3, TRITC or FITC conjugated antibodies were photographed in a dark room with a light sensitive SIT video camera (C2400-08, Hamamatsu) using a 20X water immersion objective (UMFPlanF1, Olympus), both connected to a microscope (BX50WI, Olympus). Two different filters, green (XF37) and blue-green (XF22), were used to illuminate the sections depending on whether the Cy-3/TRITC or FITC conjugated secondary antibody was used, respectively. Further processing was performed as with bright-field imaging.

2.9 Statistics

For statistical comparison of relative protein expression in different lanes on Western blots, a Wilcoxon t-test was performed. The level of significance was set to 0.05. For relative protein levels in normal muscles, the PGC-1β level in nuclear SOL fractions were set to 1.

For statistical comparison of fiber type distribution between the PGC-1β transfected, sham transfected and normal control fibers, a Fisher's exact test with Bonferroni correction was performed. The level of significance was set to 0.05. All statistical analyses were performed in GraphPad Prism 4.

3. RESULTS

3.1 PGC-1β expressionin fast and slow muscles

Western blots were performed on protein extracted from homogenized untreated EDL and SOL muscles from both legs of 18 female NMRI mice. EDL or SOL muscles from 6 animals were pooled together, respectively. This experiment was repeated three times (n=3). The homogenized samples were fractionated into cytosolic and nuclear protein and analyzed by immunoblotting. A representative blot is presented in figure 3.1A, showing a PGC-1β positive band at about 110 kDa, which corresponds to the expected size of the endogenous protein (112.1 kDa). This band was predominantly seen in the EDL nuclear fraction. As expected, the expression of the glycolysis enzyme GAPDH was higher in the glycolytic EDL than in the oxidative SOL.

A quantitative assessment was performed on three blots to measure the relative amount of endogenous PGC-1β protein in the nuclear fractions from EDL and SOL (figure 3.1B). The EDL nuclear fraction had a significantly higher relative amount of endogenous protein compared to the SOL nuclear fraction (*=$p < 0.05$, n=3). This showed that the endogenous PGC-1β is almost exclusively expressed in the EDL nuclear protein fraction of adult female NMRI mice, with 36-fold more protein, than in the SOL nuclear protein fraction. Expression of endogenous PGC-1β in the cytosolic protein fraction from SOL and EDL was not detectable.

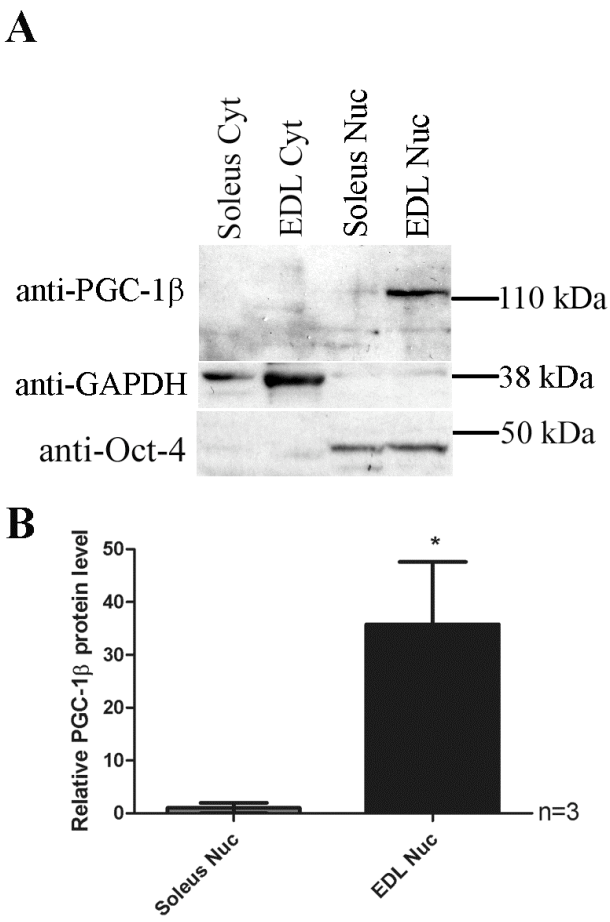

Figure 3.1 The endogenous peroxisome proliferator-activated receptor (PPAR)-gamma coactivator (PGC)-1β protein is expressed in nuclei from *extensor digitorum longus* (EDL)

A. Representative blot showing the expression of endogenous PGC-1β protein in fractionated protein samples, cytosolic (Cyt) and nuclear (Nuc), from *soleus* (SOL) and EDL. To preclude contamination of the fractionated protein samples, loading control was performed with the cytosolic marker, glyceraldehyd 3-phosphate dehydrogenase (GAPDH) and the nuclear marker Octamer (Oct)-4 transcription factor **B.** A quantitative assessment showing the relative amount of endogenous PGC-1β protein in the nuclear fractions (*=$p<0.05$), n=3. Mean ± SEM. SOL Nuc fraction set to 1.

3.2 Verification of the Flag-PGC-1β fusion protein expression

Expression of the flag-PGC-1β fusion protein was verified by transfecting HEK 293 cells with the experimental plasmid, pcDNA-f:PGC1β. As controls, non-transfected cells and cells transfected with the sham plasmid, pcDNA-f, were used. Cells were lysed, protein extracted and analyzed by Western blotting. The flag-tag is only 8 amino acids long, which corresponds to less than 1 kDa in molecular mass. The blot (figure 3.2) confirmed expression of the Flag-PGC-1β fusion protein with a band at approximately 110 kDa in the pcDNA-f:PGC-1β transfected cells, but not in the sham or non-transfected controls. This size corresponds to the predicted molecular mass of the fusion protein (approximately 113 kDa).

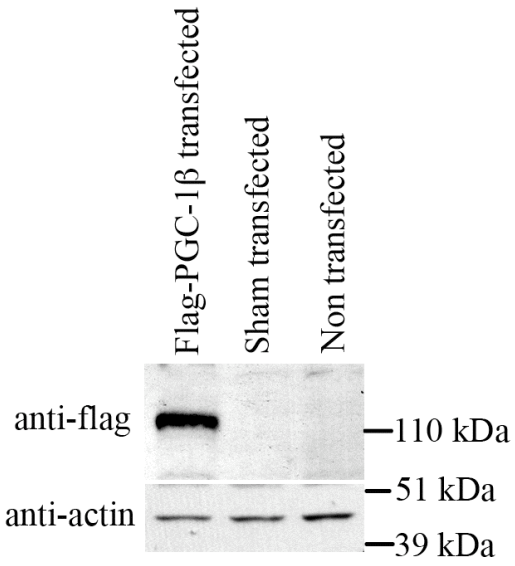

Figure 3.2 Tranfection of human embryonic kidney (HEK) 293 cells with the pcDNA-f:PGC-1β plasmid resulted in expression of the Flag-PGC-1β transgene

Protein extraction from HEK 293 cells transfected with experimental plasmid pcDNA-f:PGC-1β; sham plasmid pcDNA-f, or non-transfected presented on a Western blot. The 110 kDa band represents the flag-PGC-1β fusion protein, visualized using a flag specific antibody. Anti-actin is used as a loading control, seen at approximately 43 kDa. n=2

3.3 Effects of Flag-PGC-1β on fiber type distribution

The fiber type distribution was found by counting the number of different fiber types identified by anti-MyHC immunohistochemistry staining fourteen days after transfection. The distribution in SOL and EDL are presented in figure 3.3/table 3.1 and figure 3.4/table 3.2, respectively.

3.3.1 Fiber type distribution in SOL

A total of 1095 transfected fibers in the three groups (normal control fibers, sham transfected fibers and PGC-1β transfected fibers) from 8 female NMRI mice were analyzed (figure 3.3/table 3.1). The fiber type distribution was not significant when comparing the PGC-1β-transfected, sham-transfected and normal controls, nor between the sham-transfected and the normal control fibers (p=0.05)(figure 3.3).

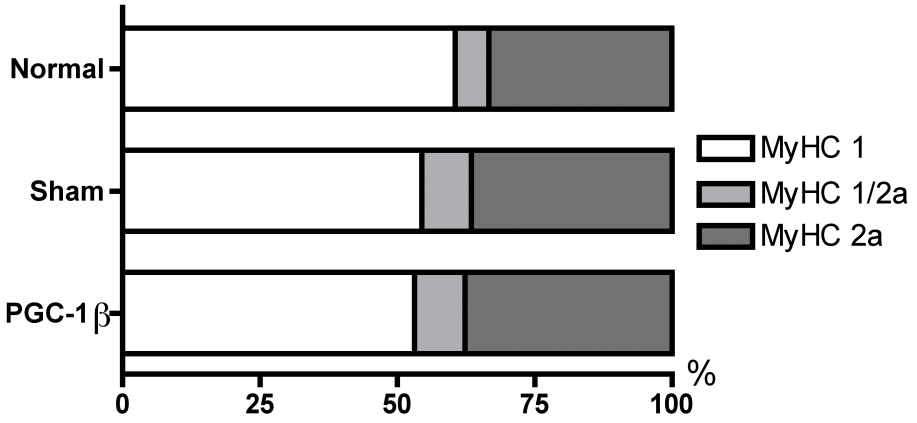

Figure 3.3 Fiber type distribution in SOL after PGC-1β transfection

Fiber type distribution in SOL in PGC-1β-transfected, sham-transfected, and normal controls (p=0.05). No significant differences were observed when comparing any of the groups. n=1095 fibers from 8 NMRI mice. For further information see table 3.2

Table 3.1 MyHC fiber type distribution in the normal control, sham-, and PGC-1β-transfected groups of SOL

Fiber type:	Normal control:		Sham transfected:		PGC-1β transfected:	
	n:	%	n:	%	n:	%
1	444	60.7	103	54.5	93	53.2
1/2a	48	6.6	17	9.0	16	19.1
2a	239	32.7	69	36.5	66	37.7
Total:	731	100	189	100	175	100

3.3.2 Fiber type distribution in EDL

A total of 2065 fibers in three groups (normal control fibers, sham-transfected fibers and PGC-1β-transfected fibers) from 8 animals were analyzed (figure 3.4/table 3.2). The fiber type distribution was significantly different when comparing PGC-1β-transfected fibers with the normal controls. There was a 33.9 % decrease in the proportion of 2a fibers (p=0.0003), and a 15.7 % increase in the proportion of 2b fibers (p=0.0004).

When comparing sham-transfected with normal controls, the proportion of 2a fibers decreased by 40.7 % (p=0.0074), the proportion of 2x fibers decreased by 48.2 % (p=0.0001) and the proportion of 2b fibers increased by 40.1 % (p<0.0001).

A significant difference in fiber type distribution was also seen when comparing the PGC-1β-transfected fibers with the sham-transfecetd fibers. There was a 17.4 % decrease in the

proportion of 2b fibers (p=0.0006) and a 77.6 % increase in the proportion of 2x fibers (p=0.0020).

As described, there was a general shift towards a faster fiber phenotype in the sham and PGC-1β transfected group when compared to the normal control. However when comparing the PGC-1β-transfected group to the sham-transfected group a drastic increase in the proportion of 2x fibers (77.6 %) at the expense of 2b fibers was evident, shifting the fiber phenotype in a slower direction.

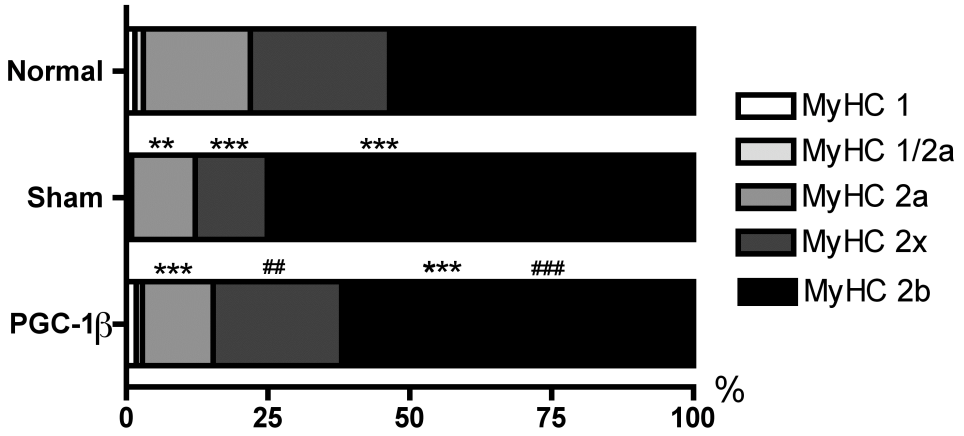

Figure 3.4 Fiber type distribution in EDL after PGC-1β transfection

Significant differences compared to the normal controls are indicated by *, while significant differences compared to the sham-transfected fibers are indicated by # (***/###=p<0.001 **/##=p<0.01). The level of significance was set to 0.05. n=2065 fibers from 8 animals. For further information see table 3.1

Table 3.2 MyHC fiber type distribution in the normal control, sham-, and PGC-1β-transfected groups of EDL

Fiber type:	Normal control:		Sham transfected:		PGC-1β transfected:	
	n:	%	n:	%	n:	%
1	18	1.5	1	0.5	12	1.8
1/2a	18	1.5	1	0.5	7	1.1
2a	226	18.9	23	11.2	83	12.5
2x	293	24.5	26	12.7	150	22.6
2b	641	53.6	154	75.1	412	62.0
Total:	1196	100	205	100	664	100

4. DISCUSSION

The present study shows that endogenous PGC-1β protein was detected exclusivly in nuclei, and not in the cytosolic fractions of either EDL or SOL. The protein was found to be expressed 36-fold higher in the fast glycolytic EDL compared to the slow oxidative SOL, while the mRNA level has been shown to be much more equal (Arany *et al.*, 2007).

The overexpression studies in EDL showed a general shift towards a slower phenotype when comparing the PGC-1β-transfected fibers with the sham-transfected fibers. This was due to a downregulation of 2b fibers and an upregulation of 2x fibers. However, when comparing both the PGC-1β-transfected and sham-transfected fibers with the non-transfected normal control, a general shift towards a faster phenotype was observed; and due to this it is difficult to interpret these results.

In SOL no significant effect was observed when comparing any of the groups, it is therefore possible to conclude that PGC-1β had no effect on MyHC expression under the experimental conditions presented in this thesis.

4.1 Subcellular localization and expression of endogenous PGC-1β

Previous experiments conducted in wild type muscles from mice have shown the expression of PGC-1β protein to be localized in nuclei by the use of *in situ* immunohistochemistry (Arany *et al.*, 2007). In accordance with Arany *et al.* (2007), PGC-1β protein was found to be expressed exclusively in the nuclear fractions from both EDL and SOL.

PGC-1β mRNA has been shown to be expressed approximately 1.6 times more in EDL than in SOL by Arany *et al.* (2007). The relative quantity of the PGC-1β protein in this study was found, as Arany *et al.* (2007) observed for mRNA, to be expressed at higher levels in EDL than in SOL. However, the difference in expression level was more extreme, with EDL expressing the PGC-1β protein 36 times more than SOL. Theoretically, this could be explained by several subcellular mechanisms such as translational efficiency or protein stability.

4.2 Effects of PGC-1β on fiber type distribution

4.2.1 "Sham effect" observed in mouse muscle

The sham group is an important control that is used to exclude possible effects of the electroporation procedure, effects of introducing foreign DNA, or overexpression of protein in general. Both the sham- and PGC-1β transfected fibers in EDL displayed a faster fiber type distribution when compared to the non-transfected normal control. We attribute the alteration in fiber type distribution to selective transfection of fast glycolytic fibers. At the present time the reason for this observed effect remains to be ascertained. However, since fast glycolytic fibers often are larger in diameter than slow oxidative fibers, and the square root of the radius (CSA) is inversely proportional to the electrical input resistance, this might be a reason for the selective transfection observed. This results in an increased conductivity through these larger fibers, thus making them less difficult to permeabilize. Electroporation is based on the principle that the applied electric field has to exceed the transmembrane threshold for any given cell to make it permeable, and this threshold is inversely proportional to cell size (Rols, 2006). If the electric field applied under our conditions is too weak to permeabilize the small fibers, a selective transfection of the large fibers, as seen here, can occur.

In SOL, however, the selective transfection was not observed. This is likely due to the more homogenous fiber size observed in SOL (e.g., Delp & Duan, 1996), which might result in a more randomized transfection of the different fiber types, rather than a selective transfection of the largest fast glycolytic fibers as observed in EDL. The fiber size of type 1 and 2a fibers in SOL have also been predicted to be larger in size than the same fibers in EDL, almost at the same size as the 2x and 2b fibers in EDL (personal communication and observations) (Delp & Duan, 1996). All of these elements coincide with the observed rate of transfection being almost equal as for that observed in EDL.

Another possible explanations for the lack of sham effect, in addition to the more homogenous fiber size, might be the geometry of the SOL muscle; compared to EDL, SOL is a flatter muscle. The electrical current per unit area of cross section (current density) will increase when the area where current is applied decreases. This results in an increased conductivity and possibly an explanation for the similar transfection rate as observed for EDL. The lack of sham

effect may also be a result of a combination of the scenarios mentioned above, not one or the other.

However, a small, non-significant tendency towards a faster phenotype can be observed when comparing both the sham- and PGC-1β-transfected fibers to the normal control in SOL. This tendency might be of significant proportions if the number of fibers transfected were to be increased. Others in our group have seen the "sham effect" in SOL, although smaller than for EDL (Hansen, 2009).

The "sham effect" has not been observed in rats (Ekmark *et al.*, 2007; Lunde *et al.*, 2007), which may be explained by the size difference, both at macroscopic and cellular levels, in mice compared to rat. The electric field applied in rats may be large enough to exceed the transmembrane threshold for all the fibers, resulting in no selective transfection, but rather a more uniform permeabilization of all fibers.

4.2.2 Effects of PGC-1β in EDL

Although no solid conclusion can be drawn from the EDL overexpression experiments due to the "sham effect", some significant differences were observed when comparing the sham- and PGC-1β-transfected fibers. This may indicate that PGC-1β overexpression could have the ability to affect MyHC expression. A faster phenotype was observed when comparing both the PGC-1β- and sham-transfected fibers to the normal control. Interestingly, when comparing the PGC-1β- and sham-transfected fibers, an increase in 2x fibers at the expense of 2b fibers was evident, resulting in a shift towards a slower phenotype. Arany *et al.* (2007) observed, in addition to downregulation of the 2b MyHC mRNA, a downregulation of the MyHC mRNA 1 and 2a at the expense of an increase of 2x in EDL in transgenic animals overexpressing PGC-1β. This is partly in agreement with the results presented in this study.

In transgenic animals overexpressing PGC-1β, the protein is present throughout both primary and secondary myofiber formation, and therefore the observed effects cannot be ruled out as the result of PGC-1β's role in myogenesis, rather than true adult muscle plasticity. Mortensen *et al.* (2006) further supports PGC-1β's role in myogenesis when they observed its involvement in the maturation of myofibers, downregulating $MyHC_{emb}$ and $MyHC_{peri}$, in cultured rat skeletal muscle myotubes. However, when the effect of PGC-1β is explored in adult mice by *in*

vivo electroporation, developmental factors are precluded from the experiment and will no longer be of influence on the results.

The PGC-1β overexpression experiments in EDL conducted in this thesis could be performed in rats, where this selective transfection has not been noted. This will probably make it less difficult to determine at which point a shift in fiber type is due solely to overexpression of the protein of interest, as opposed to any by-effects of the electroporation procedure.

4.2.3 Effects of PGC-1β in SOL

Since there were no significant differences between any of the three groups compared in SOL, this indicates that PGC-1β overexpression had no effect on MyHC expression in this muscle. This is in accordance with the observations conducted in transgenic mice (Arany *et al.*, 2007). Their PGC-1β cDNA transgene, which was cloned 3' to 4.8 kb of the promoter of muscle creatine kinase (MCK), was poorly expressed in SOL. Several studies have shown that fast-twitch muscles and glycolytic fibers contain higher levels of both MCK mRNA and MCK activity in comparison to slow-twitch muscles and oxidative fibers (Andres *et al.*, 1990; Yamashita & Yoshioka, 1991; Tsika *et al.*, 1995). Evidence also suggests that MCK promoter regulation is determined by different regulatory elements in fast- and slow-twitch fibers, resulting in an uneven expression of the gene downstream of this promoter in skeletal muscles (Johnson *et al.*, 1989; Shield *et al.*, 1996). This has also been supported by *in vivo* expression studies (Dunant *et al.*, 2003). The lack of PGC-1β expression in SOL observed by Arany *et al.* (2007) may therefore be explained by the MCK promoter's reduced activity in this muscle.

However, this argument can not be used to explain our findings, since we in this study use the CMV promoter, a "universal" virus promoter, which is not a fiber-type-restricted promoter such as the MCK promoter (Hallauer & Hastings, 2000). The lack of effect by PGC-1β on MyHC expression in SOL in our experiments has resulted in two main possible hypotheses, based on the results seen in normal non-transfected muscles. Arany *et al.* (2007) have shown that the mRNA level of PGC-1β is almost equal in both the slow muscle SOL and the fast muscle EDL in non-transfected muscles, therefore the regulation has to occur after mRNA is produced. The PGC-1β mRNA may therefore not be translated into protein or the rate of translation could be low. However, if the protein is translated, the protein might be unstable,

resulting in some form of degradation of the protein, preventing it from affecting MyHC expression. This last hypothesis is probably the most likely scenario, as most regulation occurs as a post-translational modification rather than a regulation of the translational efficiency. Again, this may also result in the degradation of the flag-PGC-1β fusion protein, resulting in no effect of transfection, as we see in this study.

Another important point to remember is, that if we are to believe the results seen in EDL when comparing the PGC-1β- and sham-transfected fibers, no effect should be observed in SOL. This is due to the lack of 2b fibers in SOL, which were the only fibers in EDL that had the ability to convert to 2x fibers.

These hypotheses show why overexpression of PGC-1β might not have any effect on MyHC expression in SOL.

4.3 Future experiments

Because of the "sham effect" observed in mouse EDL in this study, these experiments should be repeated under conditions where this selective transfection has not been observed. Then it may be clearer whether or not PGC-1β may indeed affect MyHC expression. In addition, it would be interesting to investigate possible effects of PGC-1β on the metabolic profile (SDH, GAPDH) and size (CSA) of the different fibers in adult mice compared to wild type.

In this study, PGC-1β has shown to have no effect one MyHC expression in SOL. The reason for the lack of effect by PGC-1β could easily be established by an experiment where both the mRNA and protein level were measured by homogenizing muscles electroporated with the experimental plasmid. If both mRNA and protein are present, the result of no effect is due to repression of factors involved in the transcriptional machinery or heterochromatination of target sequence. If mRNA is present, and the protein is not, this is a result of translational inefficiency or protein degradation. It is, however, not that easy to establish whether or not the lack of protein is due to degradation or translational inefficiency. Protein degradation is however a more frequent method of regulation, although this varies for molecule to molecule. If there is no mRNA present, there is a regulation at the transcriptional level. However, the presence of PGC-1β mRNA has been established by Arany *et al.* (2007). Last, but not least,

there is, off course, always a possibility that our construct might not work *in vivo,* even though it works in HEK 293 cells.

4.4 Conclusions

1. In wild type muscles, PGC-1β was exclusively found in nuclei and 36-times more in the fast glycolytic EDL muscle compared to the slow oxidative SOL muscle.

2. In EDL, overexpression of PGC-1β showed significant alterations in a slower direction, decreasing 2b fibers at the expense of an increase in 2x fibers, when comparing PGC-1β- and sham-transfected fibers. However, due to the "sham effect" no solid conclusions can be drawn without conducting the experiment in rats where this effect is not observed.

3. Overexpression of PGC-1β in SOL did not show any significant alterations in MyHC expression.

5. APPENDICES

5.1 DNA electroporation solutions

5.1.1 pcDNA-f:PGC-1 and pAP-lacZ solution (200 µl)

Solutions:	Amount:
pcDNA-f:PGC1 in H2O (2 ug/ul) (Addgene)	25 µl
pAP-lacZ in H2O (2 ug/ul)	25 µl
4 M NaCl	8 µl
dH2O	142 µl

5.1.2 pcDNA-f and pAP-lacZ solution (200 µl)

Solutions:	Amount:
pcDNA in H2O (2 ug/ul)	25 µl
pAP-lacZ in H2O (2 ug/ul)	25 µl
4 M NaCl	8 µl
dH2O	142 µl

5.2 Cell culture

5.2.1 DMEM (555 ml)

Solutions:	Amount:
DMEM (GIBCO)	500 ml
FCS (Bio Whittaker)	50 ml
Penicillin /Streptomycin (Bio Whittaker)	5 ml

5.2.2 Cell lysis buffer (2 l)

Solutions:	Amount:
50mM Trisacetate pH 7	12 g
0.27M Sucrose	184.4 g
1mM EDTA	0.75 g
1mM EGTA (ethylene glycol tetraacetic acid)	0.76 g
1mM Sodium Orthovanadate	20 ml stock
10mM B-glycerophosphate	6.3 g
50mM Sodium Fluoride	4.2 g
5mM Sodium Pyrophosphate	4.46 g
1% Triton X-100	20 ml

Make up to 2 l with distilled water. 50 µl each (per 50 ml buffer) of protease inhibitor phenylmethanesulphonylfluoride (PMSF) and Benzamide, and the same volume of β-mercaptoethanol; must be added before use.

5.3 Western blotting

5.3.1 TBS (2 l 10X) and TBS-T solution (1 l 1X)

Solutions:	Amount:
NaCl	584.4 g
Tris	48.5 g
dH_2O	2.0 l

- Dissolve NaCl and Tris in some dH2O, before adjusting the volume to 2l.
- To make TBS-T, take 100 ml of 10X TBS and 900 ml of dH2O, add 1 ml of Tween20 (P1379, Sigma Aldrich), mix well.

5.4 Histochemistry

5.4.1 PBS solution (10X)

Solutions:	Amount:
NaCl	80 g
KCl	2.0 g
Na_2HPO_4 x $2H_2O$	14.4 g
KH_2PO_4	2.0 g

- Dissolve all the chemicals in 800 ml of dH_2O
- Adjust the pH to 6.8/6.5 and the volume to 1 l
- 1X PBS solution with pH 7.4/7.1 was made up taking 100 ml of the 10X solution and 900 ml with dH_2O

5.4.2 Staining for β-galactosidase activity

- Thaw the sections to room temperature
- Make the fix solution:

Solutions:	Amount:
(Para)Formaldehyde (Electron Microscopy Sciences)	2.0 g
Gluteraldehyde (Electron Microscopy Sciences)	400 µl
10X PBS (pH 7.1)	10.0 ml
dH_2O	69.2 ml

- Dissolve the formaldehyde in dH_2O (60 °C); adjust volume to 100 ml and pH to 7.1
- Fix the sections at 4 °C for 20 min by circling the sections using a hydrophobic pen (H-4000, Vector) and applying a large drop of fix solution
- Wash the sections in 3 x 5 min in PBS (pH 7.1)

- Make the β-galactosidase staining solution:

Solutions:	Amount:
10X PBS (pH 7.1)	150 µl
0.2 M Potassium Ferro cyanide	30 µl
0.2 M Potassium Ferri cyanide	30 µl
1 M $MgCl_2$	3 µl
dH_2O	1260 µl
X-gal (50 mg I DMSO) (Promega)	30 µl

- Stain overnight at 37 °C
- Wash the sections 3 x 5 min in PBS (pH 7.1)
- Mount the sections in glycerin gel:

Solutions:	Amount:
Gelatin (PROLABO)	15 g
Glycerol (Invitrogen)	100 ml
dH_2O	100 ml

5.4.3 Staining for MyHC isoform and laminin

Staining for MyHC 1, MyHC 2a, MyHC all non-2x:

- Use a hydrophobic pen to circle the muscle section
- Dilute the primary antibody 1:2000 in 1 % bovine serum albumin (BSA) in PBS (pH 7.4)
- Incubate the sections with the primary antibody for 60 min in room temperature
- Wash the sections 3 x 5 min in PBS (pH 7.4)
- Dilute the secondary antibody 1:200 in 0.5 % BSA in PBS (pH 7.4)
- Incubate the sections with the secondary antibody for 30 min at 37 °C
- Wash the sections 3 x 5 min in PBS (pH 7.4)

Staining for MyHC 2b:

- Use a hydrophobic pen to circle the muscle section
- Dilute the primary antibody 1:2000 in 0.5 % BSA in PBS (pH 7.4)
- Incubate the sections with the primary antibody for 45 min at 37 °C
- Wash the sections 3 x 5 min in PBS (pH 7.4)
- Dilute the secondary antibody 1:300 in 0.5 % BSA in PBS (pH 7.4)
- Incubate the sections with the secondary antibody for 45 min at 37 °C
- Wash the sections 3 x 5 min in PBS (pH 7.4)

MyHC:	Primary antibody:	Secondary antibody:
1	BA-D5	Rabbit anti-mouse IgG, FITC conjugated (F-9137, SIGMA)
2a	SC-71	Rabbit anti-mouse IgG, FITC conjugated (F-9137, SIGMA)
All non-2x	BF-35	Rabbit anti-mouse IgG, FITC conjugated (F-9137, SIGMA)
2b	BF-F3	Goat anti-mouse IgM, Cy-3 (J115-165-020, Jackson ImmunoReasearch Lab)

Staining for laminin:

- Use a hydrophobic pen to circle the muscle section
- Dilute the primary antibody 1:600 in 1 % BSA in PBS (pH 7.4)
- Incubate the sections with the primary antibody for over night at 4 °C
- Wash the sections 5 x 5 min in PBS (pH 7.4)
- Dilute the secondary antibody 1:200 in 0.5 % BSA in PBS (pH 7.4)
- Incubate the sections with the secondary antibody for 60-90 min at 37 °C
- Wash the sections 5 x 5 min in PBS (pH 7.4)

Primary antibody:	Secondary antibody:
Rabbit anti-laminin (L9393, SIGMA)	Goat TRITC conjugated anti-rabbit IgG, (T6778, SIGMA)

5.5 Abbreviations

AD	Activation domain
ATP	Adenosine triphosphate
BSA	Bovine serum albumin
CaMK	Ca^{2+}/Calmodulin-dependent protein kinase
CaN	Calcineurin
CBP	CREB binding protein
cDNA	Complementary DNA
CMV	Cytomegalovirus
Co-act	Co-activator
CSA	Cross-section area
CYT	Cytosolic
CY-3	Cyanine
DHP	Dihydropyridine
DMEM	Dulbecco's modified Eagle's medium
DNA	Deoxyribonucleic acid
E	Glutamic/aspartic-rich domain
E.coli	Escherichia coli
EDL	Extensor digitorum longus
EDTA	Ethylenediaminetetraacetic
EGTA	Ethylene glycol tetraacetic acid
emb	Embryonic
ERR	Estrogen-related receptor
Eya	Eyes absent homolog
FCS	Fetal calf serum
FITC	Fluorscein
GAPDH	Glyceraldehyd 3-phosphate dehydrogenase
GPD	α-glycerophosphate dehydrogenase
HAT	Histone acetyltransferase
HBM	HCF binding domain
HCF	Host cell factor
HDAC	Histone deacetylase
HEK	Human embryonic kidney
HRP	Horse radish peroxidase
Ig	Immunoglobin
LXXLL	Leucine-rich domain
MAPK	Mitogen-activated protein kinase
mATPase	Myosin ATPase
MCK	Muscle creatine kinase
MEF	Myocyte enhancer factor
mtDNA	Mitochondrial DNA
mRNA	Messanger RNA
MyHC	Myosin heavy chain
MyLC	Myosin light chain
NFAT	Nuclear factor of activated T-cells
NRF	Nuclear respiratory factor
NUC	Nuclear
Oct	Octamer
peri	Perinatal
PBS	Phosphate buffered saline
PGC-1α	PPAR gamma coactivator-1 alpha
PGC-1β	PPAR gamma coactivator-1 beta
PPAR	Peroxisome proliferator-activated receptor
PRC	PGC-1 related coactivators
RNA	Ribonucleic acid
RRM	RNA-recognition motif
RS	Arginine/serine rich domain
RSV	Rous sarcoma virus
SDH	Succinate dehydrogenase
SDS-PAGE	Sodium dodecyl sulphate polyacrylamide gel
SEM	Standard error of mean
SERCA	Sarco/Endoplasmic reticulum Ca^{2+}-ATPase
SOL	soleus
SRC	Steroide receptor coactivator
SV	Simian virus
TBS	Tris-buffered saline
TBS-T	Tris-buffered saline with tween
TRITC	Isothiocyanate
UPC	Uncoupling protein
V	Volt
X-gal	5-bromo-4-chloro-3-indolyle-β-D-galactoside

6. REFERENCES

Akimoto T, Pohnert SC, Li P, Zhang M, Gumbs C, Rosenberg PB, Williams RS & Yan Z. (2005). Exercise stimulates PGC-1 alpha transcription in skeletal muscle through activation of the p38 MAPK pathway. *J Biol Chem* **280,** 19587-19593.

Andersson U & Scarpulla RC. (2001). PGC-1-related coactivator, a novel, serum-inducible coactivator of nuclear respiratory factor 1-dependent transcription in mammalian cells. *Mol Cell Biol* **21,** 3738-3749.

Andres V, Cusso R & Carreras J. (1990). Effect of denervation on the distribution and developmental transition of phosphoglycerate mutase and creatine phosphokinase isozymes in rat muscles of different fiber-type composition. *Differentiation* **43,** 98-103.

Arany Z. (2008). PGC-1 coactivators and skeletal muscle adaptations in health and disease. *Curr Opin Genet Dev* **18,** 426-434.

Arany Z, He H, Lin J, Hoyer K, Handschin C, Toka O, Ahmad F, Matsui T, Chin S, Wu PH, Rybkin, II, Shelton JM, Manieri M, Cinti S, Schoen FJ, Bassel-Duby R, Rosenzweig A, Ingwall JS & Spiegelman BM. (2005). Transcriptional coactivator PGC-1 alpha controls the energy state and contractile function of cardiac muscle. *Cell Metab* **1,** 259-271.

Arany Z, Lebrasseur N, Morris C, Smith E, Yang W, Ma Y, Chin S & Spiegelman BM. (2007). The transcriptional coactivator PGC-1 beta drives the formation of oxidative type IIX fibers in skeletal muscle. *Cell Metab* **5,** 35-46.

Barany M. (1967). ATPase activity of myosin correlated with speed of muscle shortening. *J Gen Physiol* **50,** Suppl:197-218.

Berchtold MW, Brinkmeier H & Muntener M. (2000). Calcium ion in skeletal muscle: its crucial role for muscle function, plasticity, and disease. *Physiol Rev* **80,** 1215-1265.

Bigard X, Sanchez H, Zoll J, Mateo P, Rousseau V, Veksler V & Ventura-Clapier R. (2000). Calcineurin Co-regulates contractile and metabolic components of slow muscle phenotype. *J Biol Chem* **275,** 19653-19660.

Biral D, Betto R, Danieli-Betto D & Salviati G. (1988). Myosin heavy chain composition of single fibres from normal human muscle. *Biochem J* **250,** 307-308.

Blaschke F, Takata Y, Caglayan E, Law RE & Hsueh WA. (2006). Obesity, peroxisome proliferator-activated receptor, and atherosclerosis in type 2 diabetes. *Arterioscler Thromb Vasc Biol* **26,** 28-40.

Bottinelli R, Betto R, Schiaffino S & Reggiani C. (1994). Maximum shortening velocity and coexistence of myosin heavy chain isoforms in single skinned fast fibres of rat skeletal muscle. *J Muscle Res Cell Motil* **15,** 413-419.

Braissant O, Foufelle F, Scotto C, Dauca M & Wahli W. (1996). Differential expression of peroxisome proliferator-activated receptors (PPARs): tissue distribution of PPAR-alpha, -beta, and -gamma in the adult rat. *Endocrinology* **137,** 354-366.

Brooke MH & Kaiser KK. (1970). Three "myosin adenosine triphosphatase" systems: the nature of their pH lability and sulfhydryl dependence. *J Histochem Cytochem* **18,** 670-672.

Buller AJ, Eccles JC & Eccles RM. (1960). Interactions between motoneurones and muscles in respect of the characteristic speeds of their responses. *J Physiol* **150,** 417-439.

Caiozzo VJ, Baker MJ & Baldwin KM. (1998). Novel transitions in MHC isoforms: separate and combined effects of thyroid hormone and mechanical unloading. *J Appl Physiol* **85,** 2237-2248.

Calabria E, Ciciliot S, Moretti I, Garcia M, Picard A, Dyar KA, Pallafacchina G, Tothova J, Schiaffino S & Murgia M. (2009). NFAT isoforms control activity-dependent muscle fiber type specification. *Proc Natl Acad Sci U S A* **106,** 13335-13340.

Cameron AR, Anton S, Melville L, Houston NP, Dayal S, McDougall GJ, Stewart D & Rena G. (2008). Black tea polyphenols mimic insulin/insulin-like growth factor-1 signalling to the longevity factor FOXO1a. *Aging Cell* **7,** 69-77.

Chin ER, Olson EN, Richardson JA, Yang Q, Humphries C, Shelton JM, Wu H, Zhu W, Bassel-Duby R & Williams RS. (1998). A calcineurin-dependent transcriptional pathway controls skeletal muscle fiber type. *Genes Dev* **12,** 2499-2509.

Delp MD & Duan C. (1996). Composition and size of type I, IIA, IID/X, and IIB fibers and citrate synthase activity of rat muscle. *J Appl Physiol* **80,** 261-270.

DeNardi C, Ausoni S, Moretti P, Gorza L, Velleca M, Buckingham M & Schiaffino S. (1993). Type 2X-myosin heavy chain is coded by a muscle fiber type-specific and developmentally regulated gene. *J Cell Biol* **123,** 823-835.

Dreyer C, Krey G, Keller H, Givel F, Helftenbein G & Wahli W. (1992). Control of the peroxisomal beta-oxidation pathway by a novel family of nuclear hormone receptors. *Cell* **68,** 879-887.

Dunant P, Larochelle N, Thirion C, Stucka R, Ursu D, Petrof BJ, Wolf E & Lochmuller H. (2003). Expression of dystrophin driven by the 1.35-kb MCK promoter ameliorates muscular dystrophy in fast, but not in slow muscles of transgenic mdx mice. *Mol Ther* **8,** 80-89.

Dunn SE, Burns JL & Michel RN. (1999). Calcineurin is required for skeletal muscle hypertrophy. *J Biol Chem* **274,** 21908-21912.

Eken T & Gundersen K. (1988). Electrical stimulation resembling normal motor-unit activity: effects on denervated fast and slow rat muscles. *J Physiol* **402,** 651-669.

Ekmark M, Gronevik E, Schjerling P & Gundersen K. (2003). Myogenin induces higher oxidative capacity in pre-existing mouse muscle fibres after somatic DNA transfer. *J Physiol* **548,** 259-269.

Ekmark M, Rana ZA, Stewart G, Hardie DG & Gundersen K. (2007). De-phosphorylation of MyoD is linking nerve-evoked activity to fast myosin heavy chain expression in rodent adult skeletal muscle. *J Physiol* **584,** 637-650.

Golzio M, Teissie J & Rols MP. (2001). Control by membrane order of voltage-induced permeabilization, loading and gene transfer in mammalian cells. *Bioelectrochemistry* **53,** 25-34.

Golzio M, Teissie J & Rols MP. (2002). Direct visualization at the single-cell level of electrically mediated gene delivery. *Proc Natl Acad Sci U S A* **99,** 1292-1297.

Gorza L, Gundersen K, Lomo T, Schiaffino S & Westgaard RH. (1988). Slow-to-fast transformation of denervated soleus muscles by chronic high-frequency stimulation in the rat. *J Physiol* **402,** 627-649.

Grifone R, Laclef C, Spitz F, Lopez S, Demignon J, Guidotti JE, Kawakami K, Xu PX, Kelly R, Petrof BJ, Daegelen D, Concordet JP & Maire P. (2004). Six1 and Eya1 expression can reprogram adult muscle from the slow-twitch phenotype into the fast-twitch phenotype. *Mol Cell Biol* **24,** 6253-6267.

Gundersen K & Eken T. (1992). The importance of frequency and amount of electrical stimulation for contractile properties of denervated rat muscles. *Acta Physiol Scand* **145,** 49-57.

Hallauer PL & Hastings KE. (2000). Human cytomegalovirus IE1 promoter/enhancer drives variable gene expression in all fiber types in transgenic mouse skeletal muscle. *BMC Genet* **1,** 1.

Handschin C, Rhee J, Lin J, Tarr PT & Spiegelman BM. (2003). An autoregulatory loop controls peroxisome proliferator-activated receptor gamma coactivator 1alpha expression in muscle. *Proc Natl Acad Sci U S A* **100,** 7111-7116.

Hansen EEH. (2009). Effects of SMPX on skeletal muscle in adult mice. *In preparation*.

Hughes SM, Chi MM, Lowry OH & Gundersen K. (1999). Myogenin induces a shift of enzyme activity from glycolytic to oxidative metabolism in muscles of transgenic mice. *J Cell Biol* **145,** 633-642.

Ianuzzo D, Patel P, Chen V, O'Brien P & Williams C. (1977). Thyroidal trophic influence on skeletal muscle myosin. *Nature* **270,** 74-76.

Izumo S, Nadal-Ginard B & Mahdavi V. (1986). All members of the MHC multigene family respond to thyroid hormone in a highly tissue-specific manner. *Science* **231,** 597-600.

Jankala H, Harjola VP, Petersen NE & Harkonen M. (1997). Myosin heavy chain mRNA transform to faster isoforms in immobilized skeletal muscle: a quantitative PCR study. *J Appl Physiol* **82,** 977-982.

Johnson JE, Wold BJ & Hauschka SD. (1989). Muscle creatine kinase sequence elements regulating skeletal and cardiac muscle expression in transgenic mice. *Mol Cell Biol* **9,** 3393-3399.

Kamei Y, Ohizumi H, Fujitani Y, Nemoto T, Tanaka T, Takahashi N, Kawada T, Miyoshi M, Ezaki O & Kakizuka A. (2003). PPARgamma coactivator 1beta/ERR ligand 1 is an

ERR protein ligand, whose expression induces a high-energy expenditure and antagonizes obesity. *Proc Natl Acad Sci U S A* **100,** 12378-12383.

Kendrew JC, Parrish RG, Marrack JR & Orlans ES. (1954). The species specificity of myoglobin. *Nature* **174,** 946-949.

Kliewer SA, Forman BM, Blumberg B, Ong ES, Borgmeyer U, Mangelsdorf DJ, Umesono K & Evans RM. (1994). Differential expression and activation of a family of murine peroxisome proliferator-activated receptors. *Proc Natl Acad Sci U S A* **91,** 7355-7359.

Klitgaard H, Ausoni S & Damiani E. (1989). Sarcoplasmic reticulum of human skeletal muscle: age-related changes and effect of training. *Acta Physiol Scand* **137,** 23-31.

Klitgaard H, Mantoni M, Schiaffino S, Ausoni S, Gorza L, Laurent-Winter C, Schnohr P & Saltin B. (1990). Function, morphology and protein expression of ageing skeletal muscle: a cross-sectional study of elderly men with different training backgrounds. *Acta Physiol Scand* **140,** 41-54.

Koulmann N & Bigard AX. (2006). Interaction between signalling pathways involved in skeletal muscle responses to endurance exercise. *Pflugers Arch* **452,** 125-139.

Koves TR, Li P, An J, Akimoto T, Slentz D, Ilkayeva O, Dohm GL, Yan Z, Newgard CB & Muoio DM. (2005). Peroxisome proliferator-activated receptor-gamma co-activator 1 alpha-mediated metabolic remodeling of skeletal myocytes mimics exercise training and reverses lipid-induced mitochondrial inefficiency. *J Biol Chem* **280,** 33588-33598.

Kressler D, Schreiber SN, Knutti D & Kralli A. (2002). The PGC-1-related protein PERC is a selective coactivator of estrogen receptor alpha. *J Biol Chem* **277,** 13918-13925.

Larsson L & Ansved T. (1995). Effects of ageing on the motor unit. *Prog Neurobiol* **45,** 397-458.

Larsson L, Edstrom L, Lindegren B, Gorza L & Schiaffino S. (1991). MHC composition and enzyme-histochemical and physiological properties of a novel fast-twitch motor unit type. *Am J Physiol* **261,** C93-101.

Lee WJ, Kim M, Park HS, Kim HS, Jeon MJ, Oh KS, Koh EH, Won JC, Kim MS, Oh GT, Yoon M, Lee KU & Park JY. (2006). AMPK activation increases fatty acid oxidation in skeletal muscle by activating PPAR alpha and PGC-1. *Biochem Biophys Res Commun* **340,** 291-295.

Lehman JJ, Barger PM, Kovacs A, Saffitz JE, Medeiros DM & Kelly DP. (2000). Peroxisome proliferator-activated receptor gamma coactivator-1 promotes cardiac mitochondrial biogenesis. *J Clin Invest* **106,** 847-856.

Lexell J. (1993). Ageing and human muscle: observations from Sweden. *Can J Appl Physiol* **18,** 2-18.

Lexell J, Downham D & Sjostrom M. (1986). Distribution of different fibre types in human skeletal muscles. Fibre type arrangement in m. vastus lateralis from three groups of healthy men between 15 and 83 years. *J Neurol Sci* **72,** 211-222.

Lexell J, Taylor CC & Sjostrom M. (1988). What is the cause of the ageing atrophy? Total number, size and proportion of different fiber types studied in whole vastus lateralis muscle from 15- to 83-year-old men. *J Neurol Sci* **84,** 275-294.

Lin J, Handschin C & Spiegelman BM. (2005). Metabolic control through the PGC-1 family of transcription coactivators. *Cell Metab* **1,** 361-370.

Lin J, Puigserver P, Donovan J, Tarr P & Spiegelman BM. (2002a). Peroxisome proliferator-activated receptor gamma coactivator 1 beta (PGC-1 beta), a novel PGC-1-related transcription coactivator associated with host cell factor. *J Biol Chem* **277,** 1645-1648.

Lin J, Tarr PT, Yang R, Rhee J, Puigserver P, Newgard CB & Spiegelman BM. (2003). PGC-1 beta in the regulation of hepatic glucose and energy metabolism. *J Biol Chem* **278,** 30843-30848.

Lin J, Wu H, Tarr PT, Zhang CY, Wu Z, Boss O, Michael LF, Puigserver P, Isotani E, Olson EN, Lowell BB, Bassel-Duby R & Spiegelman BM. (2002b). Transcriptional co-activator PGC-1 alpha drives the formation of slow-twitch muscle fibres. *Nature* **418,** 797-801.

Lojda Z. (1970). Indigogenic methods for glycosidases. II. An improved method for beta-D-galactosidase and its application to localization studies of the enzymes in the intestine and in other tissues. *Histochemie* **23,** 266-288.

Lomo T, Westgaard RH & Dahl HA. (1974). Contractile properties of muscle: control by pattern of muscle activity in the rat. *Proc R Soc Lond B Biol Sci* **187,** 99-103.

Lunde IG, Ekmark M, Rana ZA, Buonanno A & Gundersen K. (2007). PPAR delta expression is influenced by muscle activity and induces slow muscle properties in adult rat muscles after somatic gene transfer. *J Physiol* **582,** 1277-1287.

Luquet S, Lopez-Soriano J, Holst D, Fredenrich A, Melki J, Rassoulzadegan M & Grimaldi PA. (2003). Peroxisome proliferator-activated receptor delta controls muscle development and oxidative capability. *Faseb J* **17,** 2299-2301.

Mathiesen I. (1999). Electropermeabilization of skeletal muscle enhances gene transfer in vivo. *Gene Ther* **6,** 508-514.

McGee SL & Hargreaves M. (2004). Exercise and myocyte enhancer factor 2 regulation in human skeletal muscle. *Diabetes* **53,** 1208-1214.

McKinsey TA, Zhang CL, Lu J & Olson EN. (2000). Signal-dependent nuclear export of a histone deacetylase regulates muscle differentiation. *Nature* **408,** 106-111.

McKinsey TA, Zhang CL & Olson EN. (2002). MEF2: a calcium-dependent regulator of cell division, differentiation and death. *Trends Biochem Sci* **27,** 40-47.

Mercier J, Perez-Martin A, Bigard X & Ventura R. (1999). Muscle plasticity and metabolism: effects of exercise and chronic diseases. *Mol Aspects Med* **20,** 319-373.

Michael LF, Wu Z, Cheatham RB, Puigserver P, Adelmant G, Lehman JJ, Kelly DP & Spiegelman BM. (2001). Restoration of insulin-sensitive glucose transporter (GLUT4) gene expression in muscle cells by the transcriptional coactivator PGC-1. *Proc Natl Acad Sci U S A* **98,** 3820-3825.

Mootha VK, Handschin C, Arlow D, Xie X, St Pierre J, Sihag S, Yang W, Altshuler D, Puigserver P, Patterson N, Willy PJ, Schulman IG, Heyman RA, Lander ES & Spiegelman BM. (2004). Erralpha and Gabpa/b specify PGC-1 alpha-dependent oxidative phosphorylation gene expression that is altered in diabetic muscle. *Proc Natl Acad Sci U S A* **101,** 6570-6575.

Mortensen OH, Frandsen L, Schjerling P, Nishimura E & Grunnet N. (2006). PGC-1 alpha and PGC-1 beta have both similar and distinct effects on myofiber switching toward an oxidative phenotype. *Am J Physiol Endocrinol Metab* **291,** E807-816.

Moxley RT, 3rd. (1994). Potential for growth factor treatment of muscle disease. *Curr Opin Neurol* **7,** 427-434.

Needham D. (1926). Red and white muscle. *Physiological Reviews* **6,** 1-27.

Noirez P, Torres S, Cebrian J, Agbulut O, Peltzer J, Butler-Browne G, Daegelen D, Martelly I, Keller A & Ferry A. (2006). TGF-beta1 favors the development of fast type identity during soleus muscle regeneration. *J Muscle Res Cell Motil* **27,** 1-8.

Nwoye L & Mommaerts WF. (1981). The effects of thyroid status on some properties of rat fast-twitch muscle. *J Muscle Res Cell Motil* **2,** 307-320.

Okumura N, Hashida-Okumura A, Kita K, Matsubae M, Matsubara T, Takao T & Nagai K. (2005). Proteomic analysis of slow- and fast-twitch skeletal muscles. *Proteomics* **5,** 2896-2906.

Oliver WR, Jr., Shenk JL, Snaith MR, Russell CS, Plunket KD, Bodkin NL, Lewis MC, Winegar DA, Sznaidman ML, Lambert MH, Xu HE, Sternbach DD, Kliewer SA, Hansen BC & Willson TM. (2001). A selective peroxisome proliferator-activated receptor delta agonist promotes reverse cholesterol transport. *Proc Natl Acad Sci U S A* **98,** 5306-5311.

Pattullo MC, Cotter MA, Cameron NE & Barry JA. (1992). Effects of lengthened immobilization on functional and histochemical properties of rabbit tibialis anterior muscle. *Exp Physiol* **77,** 433-442.

Paukal E. (1904). Die Zuckungsformen von Kaninchen Muskeln verschiedener Farbe und Struktur. *Arch Anat Physiol* **2,** 100-120.

Personius KE & Balice-Gordon RJ. (2001). Loss of correlated motor neuron activity during synaptic competition at developing neuromuscular synapses. *Neuron* **31,** 395-408.

Pette D. (2002). The adaptive potential of skeletal muscle fibers. *Can J Appl Physiol* **27,** 423-448.

Pette D & Staron RS. (1990). Cellular and molecular diversities of mammalian skeletal muscle fibers. *Rev Physiol Biochem Pharmacol* **116,** 1-76.

Pette D & Staron RS. (1993). The Molecular Diversity of Mammalian Muscle Fibers. *News Physiol Sci* **8,** 153-157.

Pette D & Staron RS. (1997). Mammalian skeletal muscle fiber type transitions. *Int Rev Cytol* **170,** 143-223.

Pette D & Staron RS. (2000). Myosin isoforms, muscle fiber types, and transitions. *Microsc Res Tech* **50,** 500-509.

Pette D & Vrbova G. (1985). Neural control of phenotypic expression in mammalian muscle fibers. *Muscle Nerve* **8,** 676-689.

Puigserver P, Adelmant G, Wu Z, Fan M, Xu J, O'Malley B & Spiegelman BM. (1999). Activation of PPAR gamma coactivator-1 through transcription factor docking. *Science* **286,** 1368-1371.

Puigserver P, Wu Z, Park CW, Graves R, Wright M & Spiegelman BM. (1998). A cold-inducible coactivator of nuclear receptors linked to adaptive thermogenesis. *Cell* **92,** 829-839.

Rana ZA, Ekmark M & Gundersen K. (2004). Coexpression after electroporation of plasmid mixtures into muscle in vivo. *Acta Physiol Scand* **181,** 233-238.

Rana ZA, Gundersen K & Buonanno A. (2008). Activity-dependent repression of muscle genes by NFAT. *Proc Natl Acad Sci U S A* **105,** 5921-5926.

Ranvier L. (1874). De quelques faits relatifs a l'histologie et a la physiologie des muscles stries. *Arch Physiol Norm Pathol* **1,** 5-10.

Rao A, Luo C & Hogan PG. (1997). Transcription factors of the NFAT family: regulation and function. *Annu Rev Immunol* **15,** 707-747.

Reiser PJ, Moss RL, Giulian GG & Greaser ML. (1985). Shortening velocity in single fibers from adult rabbit soleus muscles is correlated with myosin heavy chain composition. *J Biol Chem* **260,** 9077-9080.

Rivero JL, Talmadge RJ & Edgerton VR. (1998). Fibre size and metabolic properties of myosin heavy chain-based fibre types in rat skeletal muscle. *J Muscle Res Cell Motil* **19,** 733-742.

Rols MP. (2006). Electropermeabilization, a physical method for the delivery of therapeutic molecules into cells. *Biochim Biophys Acta* **1758,** 423-428.

Rols MP & Teissie J. (1990). Electropermeabilization of mammalian cells. Quantitative analysis of the phenomenon. *Biophys J* **58,** 1089-1098.

Roos MR, Rice CL & Vandervoort AA. (1997). Age-related changes in motor unit function. *Muscle Nerve* **20,** 679-690.

Rosen ED & Spiegelman BM. (2000). Molecular regulation of adipogenesis. *Annu Rev Cell Dev Biol* **16,** 145-171.

Sanes JR, Rubenstein JL & Nicolas JF. (1986). Use of a recombinant retrovirus to study post-implantation cell lineage in mouse embryos. *Embo J* **5,** 3133-3142.

Scarpulla RC. (2002). Nuclear activators and coactivators in mammalian mitochondrial biogenesis. *Biochim Biophys Acta* **1576,** 1-14.

Scarpulla RC. (2006). Nuclear control of respiratory gene expression in mammalian cells. *J Cell Biochem* **97,** 673-683.

Schiaffino S, Gorza L, Sartore S, Saggin L, Ausoni S, Vianello M, Gundersen K & Lomo T. (1989). Three myosin heavy chain isoforms in type 2 skeletal muscle fibres. *J Muscle Res Cell Motil* **10,** 197-205.

Schiaffino S, Gorza L, Sartore S, Saggin L & Carli M. (1986). Embryonic myosin heavy chain as a differentiation marker of developing human skeletal muscle and rhabdomyosarcoma. A monoclonal antibody study. *Exp Cell Res* **163,** 211-220.

Schiaffino S & Reggiani C. (1994). Myosin isoforms in mammalian skeletal muscle. *J Appl Physiol* **77,** 493-501.

Schiaffino S & Reggiani C. (1996). Molecular diversity of myofibrillar proteins: gene regulation and functional significance. *Physiol Rev* **76,** 371-423.

Schiaffino S, Sandri M & Murgia M. (2007). Activity-dependent signaling pathways controlling muscle diversity and plasticity. *Physiology (Bethesda)* **22,** 269-278.

Schmidt A, Endo N, Rutledge SJ, Vogel R, Shinar D & Rodan GA. (1992). Identification of a new member of the steroid hormone receptor superfamily that is activated by a peroxisome proliferator and fatty acids. *Mol Endocrinol* **6,** 1634-1641.

Seward DJ, Haney JC, Rudnicki MA & Swoap SJ. (2001). bHLH transcription factor MyoD affects myosin heavy chain expression pattern in a muscle-specific fashion. *Am J Physiol Cell Physiol* **280,** C408-413.

Shield MA, Haugen HS, Clegg CH & Hauschka SD. (1996). E-box sites and a proximal regulatory region of the muscle creatine kinase gene differentially regulate expression in

diverse skeletal muscles and cardiac muscle of transgenic mice. *Mol Cell Biol* **16,** 5058-5068.

Sieck GC, Zhan WZ, Prakash YS, Daood MJ & Watchko JF. (1995). SDH and actomyosin ATPase activities of different fiber types in rat diaphragm muscle. *J Appl Physiol* **79,** 1629-1639.

Spangenburg EE & Booth FW. (2003). Molecular regulation of individual skeletal muscle fibre types. *Acta Physiol Scand* **178,** 413-424.

St-Pierre J, Lin J, Krauss S, Tarr PT, Yang R, Newgard CB & Spiegelman BM. (2003). Bioenergetic analysis of peroxisome proliferator-activated receptor gamma coactivators 1 alpha and 1 beta (PGC-1 alpha and PGC-1 beta) in muscle cells. *J Biol Chem* **278,** 26597-26603.

Staron RS, Hagerman FC, Hikida RS, Murray TF, Hostler DP, Crill MT, Ragg KE & Toma K. (2000). Fiber type composition of the vastus lateralis muscle of young men and women. *J Histochem Cytochem* **48,** 623-629.

Tontonoz P, Hu E, Graves RA, Budavari AI & Spiegelman BM. (1994a). mPPAR gamma 2: tissue-specific regulator of an adipocyte enhancer. *Genes Dev* **8,** 1224-1234.

Tontonoz P, Hu E & Spiegelman BM. (1994b). Stimulation of adipogenesis in fibroblasts by PPAR gamma 2, a lipid-activated transcription factor. *Cell* **79,** 1147-1156.

Tsika RW, Hauschka SD & Gao L. (1995). M-creatine kinase gene expression in mechanically overloaded skeletal muscle of transgenic mice. *Am J Physiol* **269,** C665-674.

Van Zyl CG, Noakes TD & Lambert MI. (1995). Anabolic-androgenic steroid increases running endurance in rats. *Med Sci Sports Exerc* **27,** 1385-1389.

Vega RB, Huss JM & Kelly DP. (2000). The coactivator PGC-1 cooperates with peroxisome proliferator-activated receptor alpha in transcriptional control of nuclear genes encoding mitochondrial fatty acid oxidation enzymes. *Mol Cell Biol* **20,** 1868-1876.

Vianna CR, Huntgeburth M, Coppari R, Choi CS, Lin J, Krauss S, Barbatelli G, Tzameli I, Kim YB, Cinti S, Shulman GI, Spiegelman BM & Lowell BB. (2006). Hypomorphic mutation of PGC-1beta causes mitochondrial dysfunction and liver insulin resistance. *Cell Metab* **4,** 453-464.

Vrbova G. (1963). The effect of motorneurone activity on the speed of contraction of striated muscle. *J Physiol* **169,** 513-526.

Wang YX, Lee CH, Tiep S, Yu RT, Ham J, Kang H & Evans RM. (2003). Peroxisome-proliferator-activated receptor delta activates fat metabolism to prevent obesity. *Cell* **113,** 159-170.

Wang YX, Zhang CL, Yu RT, Cho HK, Nelson MC, Bayuga-Ocampo CR, Ham J, Kang H & Evans RM. (2004). Regulation of muscle fiber type and running endurance by PPARdelta. *PLoS Biol* **2,** e294.

Wernig A, Irintchev A & Weisshaupt P. (1989). Muscle Injury, Cross-sectional Area and Fiber Type Distribution in Mouse Soleus After Intermittent Wheel-running. *J Physiol* **428,** 639-652.

Westgaard RH & Lomo T. (1988). Control of contractile properties within adaptive ranges by patterns of impulse activity in the rat. *J Neurosci* **8,** 4415-4426.

Willson TM, Brown PJ, Sternbach DD & Henke BR. (2000). The PPARs: from orphan receptors to drug discovery. *J Med Chem* **43,** 527-550.

Windisch A, Gundersen K, Szabolcs MJ, Gruber H & Lomo T. (1998). Fast to slow transformation of denervated and electrically stimulated rat muscle. *J Physiol* **510 (Pt 2),** 623-632.

Wright DC, Han DH, Garcia-Roves PM, Geiger PC, Jones TE & Holloszy JO. (2007). Exercise-induced mitochondrial biogenesis begins before the increase in muscle PGC-1 alpha expression. *J Biol Chem* **282,** 194-199.

Wu H, Naya FJ, McKinsey TA, Mercer B, Shelton JM, Chin ER, Simard AR, Michel RN, Bassel-Duby R, Olson EN & Williams RS. (2000). MEF2 responds to multiple calcium-regulated signals in the control of skeletal muscle fiber type. *Embo J* **19,** 1963-1973.

Wu Z, Puigserver P, Andersson U, Zhang C, Adelmant G, Mootha V, Troy A, Cinti S, Lowell B, Scarpulla RC & Spiegelman BM. (1999). Mechanisms controlling mitochondrial biogenesis and respiration through the thermogenic coactivator PGC-1. *Cell* **98,** 115-124.

Xu HE, Lambert MH, Montana VG, Parks DJ, Blanchard SG, Brown PJ, Sternbach DD, Lehmann JM, Wisely GB, Willson TM, Kliewer SA & Milburn MV. (1999). Molecular recognition of fatty acids by peroxisome proliferator-activated receptors. *Mol Cell* **3,** 397-403.

Yamashita K & Yoshioka T. (1991). Profiles of creatine kinase isoenzyme compositions in single muscle fibres of different types. *J Muscle Res Cell Motil* **12,** 37-44.

Zhao M, New L, Kravchenko VV, Kato Y, Gram H, di Padova F, Olson EN, Ulevitch RJ & Han J. (1999). Regulation of the MEF2 family of transcription factors by p38. *Mol Cell Biol* **19,** 21-30.